1971

Creep recovery of rutile under reduced stress

Vinjamuri Krishnamachari
Iowa State University

Creep recovery of rutile under reduced stress

by

Vinjamuri Krishnamachari

A Dissertation Submitted to the

Graduate Faculty in Partial Fulfillment of

The Requirements for the Degree of

DOCTOR OF PHILOSOPHY

Major Subject: Nuclear Engineering

Approved:

Signature was redacted for privacy.

In Charge of Major Work

Signature was redacted for privacy.

For the Major Department

Signature was redacted for privacy.

For the Graduate College

Iowa State University
Ames, Iowa

1971

TABLE OF CONTENTS

I. INTRODUCTION

The ability of materials to resist high-temperature creep deformation is technologically important. For example, the creep behavior of materials used for high temperature refractories and turbine blades can limit the service lives of those components. As a result of the importance of creep a large body of creep information [14,16,31], has been accumulated under conditions of constant temperature and stress for pure metals, various alloys, and to a lesser extent ceramic materials. Much less information is available, however, on the effects of varying stresses on the creep behavior of metals and ceramics. Since this is an area of importance in many high temperature applications, much work remains to be done if an understanding of various rate controlling mechanisms and parameters is to be attained.

Dorn and co-workers [36,44], studied the effect of stress variations on the creep deformation in pure aluminum. They observed that a cyclic stress treatment $\sigma_o \rightarrow \sigma_r$ $(< \sigma_o) \rightarrow \sigma_o$ where, σ_o is the initial creep stress and σ_r is a reduced stress, would result in the recovery of creep resistant substructure. They attributed this phenomena to the migration of sub-boundaries and subsequent sweeping out of dislocation barriers during the reduced stress periods. Similar investigations on pure lead by Kennedy [30] and Bull [7] have also revealed creep recovery. Kennedy [30] concluded that the recovery process provides the nuclei for recrystallization. Bull [7] reported that the activation energy for recovery is within 2 percent of the value for grain boundary migration reported by Gifkins [18]. In dilute Al-Mg solid solution, however,

Bell [3] found no such recovery, a phenomenon which he attributed to subgrain boundary pinning by Mg atoms.

A similar study of the recovery of creep resistant substructure in rutile single crystals ($\sigma_o \rightarrow \sigma_r \rightarrow \sigma_o$, where σ_o = 10,000 psi, and σ_r = 500 psi) was made by Bell, Krishnamachari and Jones [6]. They obtained an activation energy of 135 kcal/mole for the recovery process. They suggested that the primary mechanism for the recovery of creep resistant substructure involves the migration of subboundaries and subsequent sweeping out of dislocation barriers during the reduced stress periods.

The purpose of this investigation was to study the effect of various reduced stresses on the recovery of creep resistant substructures in rutile single crystals.

II. REVIEW OF LITERATURE

A. A General Description of Creep Behavior

ASTM E_6 defines creep as the "time-dependent part of strain resulting from force." The primary independent variables of creep deformation are stress and temperature.

A typical creep curve is shown in Figure 1. In the general case a creep curve consists of four stages: stage 1, termed the instantaneous strain, represents the strain which occurs upon loading; stage 2, termed primary or transient creep, represents the initial region of decreasing creep rate; stage 3, termed secondary or steady state creep, represents the region of relatively constant creep rate; and finally stage 4, termed tertiary creep, represents the final region of increasing creep rate, which leads eventually to specimen failure.

In general, during creep of materials one can consider that two types of processes operate: one increases resistance to flow (strain hardening); the other decreases the resistance (recovery). If hardening predominates, the creep rate continually decreases (primary creep); a balance between hardening and recovery yields a constant creep rate (steady state creep). Usually the increase in creep rate in the tertiary stage is due to an increase in stress as the area is reduced either by necking down of the specimen or by internal fracture or void formation. It may also be due to metallurgical changes, such as recrystallization or overaging.

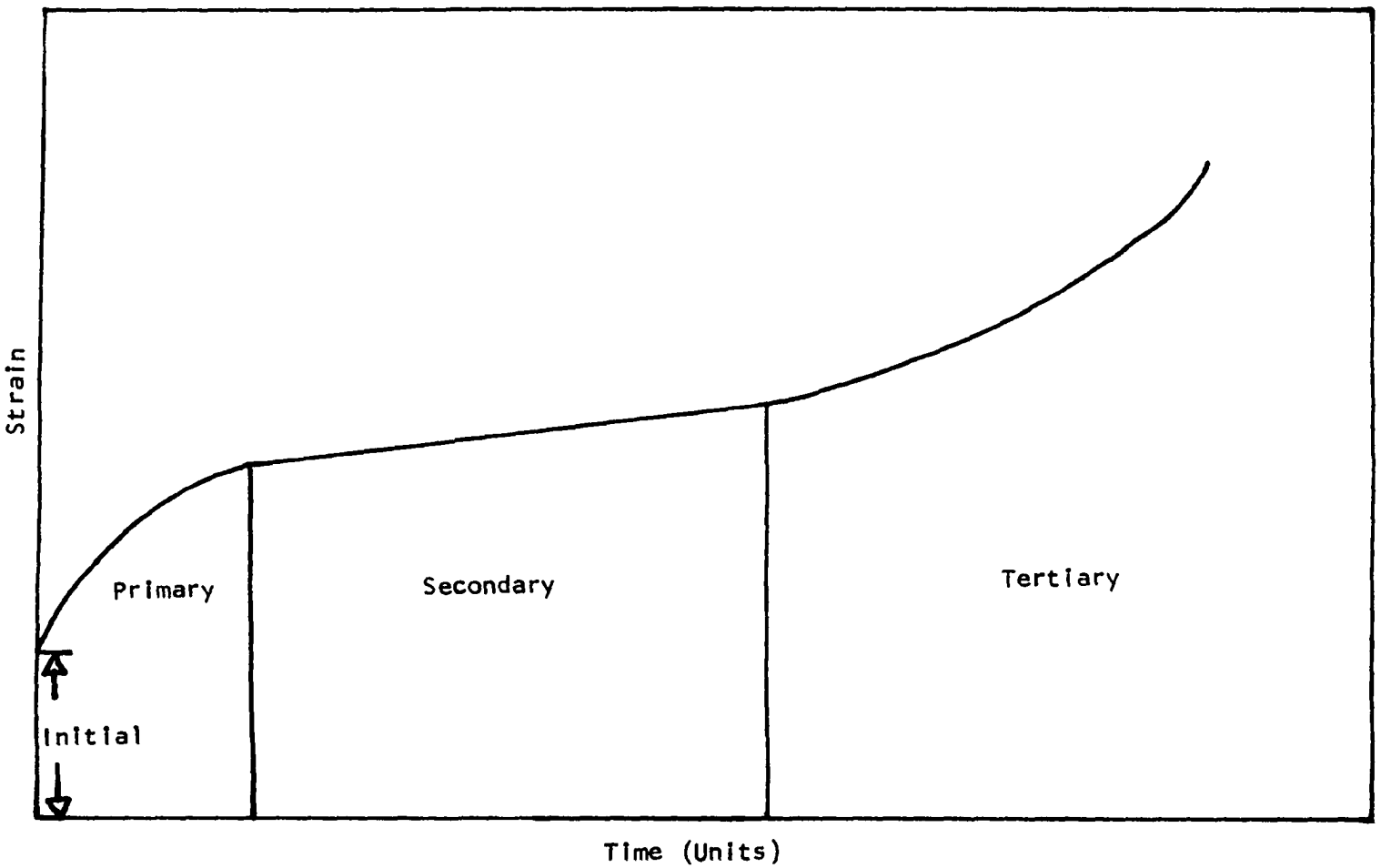

Figure 1. Characteristic creep curve

B. Stress Dependence of Secondary Creep Rate

For metals, alloys and ceramics in the annealed condition tested at constant temperature, the stress dependence of secondary creep rate $\dot{\epsilon}_s$ at low stress levels is given by the power relation

$$\dot{\epsilon}_s = A\,\sigma^m \tag{1}$$

where the stress, σ, is held constant and A and m are independent of stress. For annealed metals and alloys, m has been found to range from 1 to 7 and does not seem to depend on crystal structure [16]. A, and to some extent m, are dependent on temperature [16]. Under conditions where creep may be controlled by stress induced migration of vacancies at temperatures near the melting point, m approaches 1. Under normal conditions m typically lies between 4 and 6 for pure metals, between 2 and 4 for alloys, and from 1 to 7 for ceramic oxides [32].

At relatively high stress levels the stress dependence of secondary creep rate is given by

$$\dot{\epsilon}_s = A' \exp(\beta\sigma) \tag{2}$$

where A' and β are independent of stress. This relation has been satisfied for single crystals and polycrystals of annealed metals and alloys. A' and β are found to depend on temperature [16]. Equations (1) and (2) are satisfied by a single stress function [16], given by

$$\dot{\epsilon}_s = A'' (\sinh\ \alpha\sigma)^m \tag{3}$$

where A'' and α are constant at a given temperature. For values of $\alpha\sigma < 0.8$, Equation (3) reduces to Equation (1) and $A''\,\alpha^m = A$. For values

of $\alpha\sigma > 1.2$, Equation (3) reduces to Equation (2). Therefore, $A''/2^m = A'$ and $m\alpha = \beta$. Equation (3) gives a good representation for the steady state creep rate of many metals and alloys.

In determining the stress dependence of the creep rate at constant temperature no effort usually is made to maintain a constant structure. As creep progresses into the primary stage, structural changes occur, particularly in terms of numbers and arrangements of dislocations. In reality the true stress dependence can only be determined if the structure remains constant. Taking structure into consideration the creep rate dependence at low stress is given by

$$\dot{\epsilon}\, e^{\Delta H_c/RT} = S'\, \sigma^m \qquad (4)$$

where ΔH_c is the activation energy for creep, m is the stress exponent and S' is the structure parameter [16]. The structure parameter S' accounts for the arrangement and density of dislocations, the type and dispersion of precipitates, the grain size or type of grain and the number of subboundaries, etc. The value of m is in the range of 2 to 4 for alloys [16]. The maximum change in S' with creep strain amounts to about a factor of two and is relatively insensitive to stress [47]. Since S' is relatively insensitive to stress, the structure remains relatively constant at constant strain and the creep rate for a given material depends only on the instantaneous value of the stress, strain, and temperature.

At high stresses the relation between creep rate, structure parameter and stress is given by

$$\dot{\epsilon}\, e^{\Delta H_c/RT} = S'' \exp(\beta' \sigma) \tag{5}$$

where S'' is the structure parameter and ΔH_c and β' are independent of temperature (from about 0.45 Tm to 0.65 Tm) prior history and stress [47]. Although β' is insensitive to temperature over a limited range, prior stress history, and stress, it is sensitive to alloy additions. The variation of S'' with creep strain and stress for aluminum was discussed by Sherby et al. [47]. They found that the structure parameter S'' decreases rapidly with creep strain during primary creep and reaches a constant value during secondary creep. For aluminum this parameter is very sensitive to the stress level indicating development of different structures at different stresses.

C. Temperature Dependence of Creep

The majority of creep experiments show that creep involves thermally activated rate processes. The creep rate depends on the temperature in the form

$$\exp(-\Delta H_i/RT)$$

where ΔH_i is the activation energy of the ith deformation process. The creep rate can be generally expressed in the form

$$\dot{\epsilon}_i = \sum_i f_i(\sigma, T, S) \exp\left[\frac{-\Delta H_i(\sigma, T, S)}{RT}\right] \tag{6}$$

where f_i is the frequency factor, ΔH_i is the activation energy for the ith process, R is the gas constant, T is the absolute temperature, ^{o}K, and S is the structure term. In many cases the mechanism controlling creep may be surmised by comparing the apparent activation energy ΔH_c

with ΔH_i for likely control mechanisms. The experimental determination of ΔH_c is based on the assumption that f_i remain constant within small temperature intervals at constant stress and creep strain and that the activation energy is not stress dependent. Several methods for determining ΔH_c are described by Garofalo [16].

The creep of metals and alloys is often arbitrarily separated into low temperature (< 0.5 Tm) and high temperature (> 0.5 Tm) behavior. At low temperatures, creep is believed to be governed by non-diffusion-controlled mechanisms namely, cross slip, intersection of dislocations, and lattice friction ("peierls force"). At high temperatures creep is believed to be governed by diffusion controlled mechanisms. It has been established for many metals that at high temperatures the diffusion controlled mechanisms governing creep involve self diffusion. The coefficient of self diffusion, D_s, is given by

$$D_s = D_o \exp\left(\frac{-\Delta H_d}{RT}\right) \qquad (7)$$

where ΔH_d is the activation energy for self diffusion. For pure metals at high temperatures, ΔH_c is nearly equal to the activation energy for self diffusion, ΔH_d [13]. For alloys and ionic materials ΔH_c in many cases is nearly equal to the activation energy for diffusion of one of the elements, usually the one exhibiting the lowest diffusivity [16]. The dependence of ΔH_c on temperature, creep deformation, stress, composition and structure is well documented in the literature [16]. Since creep depends on thermally activated rate processes, it is likely that for many of these processes the applied stress will tend to assist the

thermal energy in overcoming the barriers for deformation. The apparent activation energy is given by

$$\Delta H_c = \Delta H_i - V f(\sigma) \tag{8}$$

where ΔH_i is the true activation energy, V is the activation volume, and σ is the applied stress. The activation volume V is equal to $10^2 - 10^4\, b^3$ for the non-conservative motion of jogs and to b^3 for the climb process [11], where b is the Burgers vector.

Many investigations [13,16] have shown that for pure metals and dilute solid solutions the effect of temperature variations on high temperature creep curves can be represented by the functional relationship:

$$\epsilon = f(\theta_c),\ \sigma = \text{constant} \tag{9}$$

where

ϵ = total creep strain

θ_c = temperature compensated time, $\int_o^t e^{-\Delta H_c/RT}\, dt$

f = function of θ_c which also depends on creep stress, σ

t = time under stress, and

σ = creep stress.

The validity of this correlation for high purity aluminum was demonstrated by Dorn [12]. Creep was conducted under a stress 3,000 psi at three different temperatures 531, 478 and 424°K as shown in Figure 2. When the creep strain was plotted against $\theta_c = t\, e^{-34000/RT}$, all the data points lay on the same curve as shown in Figure 3. Figure 3 confirms the validity of the Equation (9). Bell, Krishnamachari and Jones [5] have also confirmed

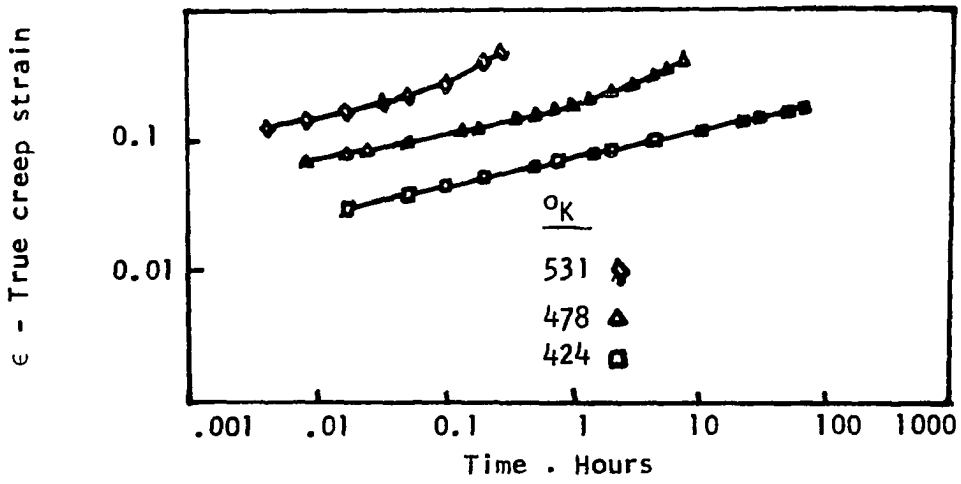

Figure 2. Creep curves for high purity aluminum under a constant true stress of 3,000 psi (Dorn [12])

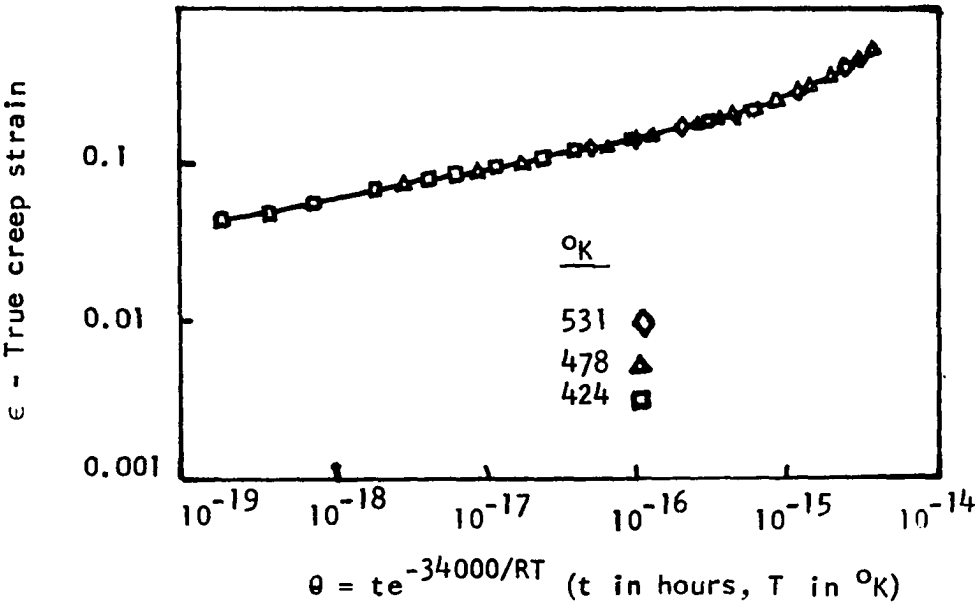

Figure 3. Creep strain as a function of the temperature compensated time for a constant true stress of 3,000 psi (Dorn [12])

that the functional relationship of Equation (9) holds true for [illegible].

D. Subgrain Formation During Creep

In general subgrains are formed during creep by polygonization. Cahn [8] reported the results of a study on the effects of annealing bent single crystals of zinc, aluminum, magnesium, and sodium chloride. His work provided the first clear picture of polygonization. Crystals were bent about an axis parallel to their active slip planes, after which transmission Laue patterns were taken with the X-ray beam normal to these planes. The patterns revealed the expected continuous asterisms. When a bent crystal was annealed and a second Laue pattern taken, the continuous asterisms became discontinuous. Cahn explained the break up of the asterisms due to the formation of dislocation walls perpendicular to the active slip plane as shown in Figure 4. These dislocation walls, if made up of edge dislocations of one sign arranged above another, would have a lower total elastic strain energy than would the more random dislocation arrangement before annealing. This lowering of strain energy provides the driving force for the process. Both glide and climb of edge dislocations are required to form the walls. First, the dislocations are distributed along the glide planes by a thermally-induced glide process. Next, the dislocations of opposite sign are cancelled forming dislocation walls which are made up of edge dislocations of the same sign.

The earliest work of Wood and his collaborators [59,60,61] brought evidence that the subgrain structure is closely related to the variables of creep such as strain, temperature, and stress. Shepard and Dorn [46]

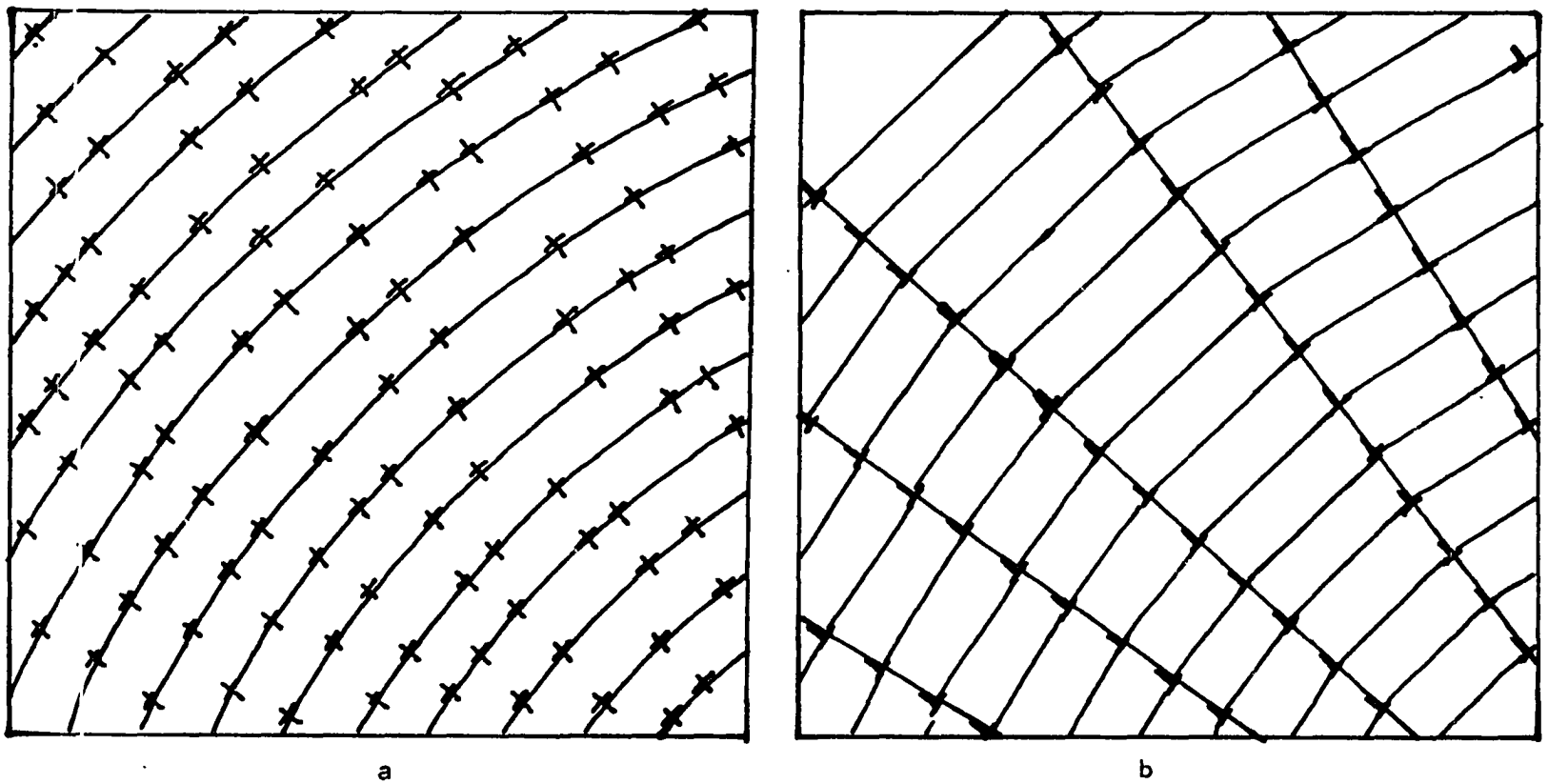

Figure 4. Disposition of edge dislocations in a bent single crystal, (a) As bent, (b) Annealed. [8]

noted that the subgrain sizes during the primary and secondary stages of creep are independent of the test temperature and strain. They also noted that the angle between adjacent subgrains continued to increase uniformly throughout the primary and secondary stages of creep. Consequently the disorientation of subgrains does not affect the secondary creep rate.

As sub-boundary formation occurs by a process of dislocation climb requiring diffusion of vacancies to the dislocations, they were able to demonstrate that the substructure generated over the primary as well as the secondary stage of creep could be related by the temperature compensated time parameter, θ_c, as described in page 9 . Thus, at one stress, the subgrain structure is constant for equal values of strain or of θ_c, the temperature compensated time.

McLean [40], Servi, Norton and Grant [45], and Shepard and Dorn [46], have studied on the stress dependence of the subgrain size. They obtained a relative estimate of the variation of subgrain diameter d, with stress σ. This relation for high purity aluminum is approximately given by

$$d = K \sigma^{-3/4} \qquad (10)$$

where

d = subgrain diameter

K = constant

σ = stress.

There is evidence that indicates that the ease of cell or subgrain formation decreases as the stacking fault energy decreases [49]. As the stacking fault energy is lowered the separation between dislocation

partials increases, and climb is inhibited. Alloying in many cases decreases stacking fault energy and subgrain formation becomes less prominent. In general metals with high stacking fault energy such as Al, α-Fe, Mg and Sn show a pronounced tendency toward subgrain formation [16]. Zinc and Cadmium which have low stacking fault energy, also show tendency for subgrain formation. Copper which exhibits intermediate stacking fault energy shows a low tendency toward subgrain formation, and lead which has low stacking fault energy, does not exhibit subgrain formation.

E. Dislocation Creep Models

The most widely accepted dislocation creep models are

1. The motion of jogged screw dislocations, and
2. The climb of edge dislocations.

1. Motion of jogged screw dislocations

Mott [41] was the first investigator to formulate a theory of high temperature creep based on the motion of jogged screw dislocations. When a screw dislocation cuts another screw dislocation a jog forms which cannot move with the dislocation without leaving a trail of vacancies or interstitial atoms behind it. This type of jog is called a non-conservative jog. Generation of vacancies is preferred during the movement of the short-edge segment which constitutes the jog because the energy of formation of a vacancy is lower. The vacancies restrain the movement of jogged dislocations unless the vacancies can move away from the jog. According to the vacancy absorption model [42], the secondary shear strain

rate is given by

$$\dot{\gamma} = \rho_s \, 6 \, D \left(1 - e^{\frac{-\tau \ell_j b^2}{RT}}\right) \qquad (11)$$

where the terms ρ_s, τ, ℓ_j, b and D refer respectively to the density of mobile screw dislocations, the applied Shear stress, the mean distance between jogs, the Burgers vector and diffusivity coefficient.

One of the difficulties encountered in using this model is the prediction of stress dependence of creep. At low values of stress, when $\tau \ell_j b^2/RT$ is small, the above equation for shear strain rate reduces to $\dfrac{\rho_s \, 6 \, D \, \tau \, \ell_j \, b^2}{RT}$.

In order to arrive at the observed stress power law for creep it follows that ρ_s must increase approximately as τ^{m-1}, if a reasonable assumption is made that ℓ_j is independent of stress. But it is expected that ρ_s is a fraction of ρ of Equation (12) [42],

$$\frac{\tau}{2} = \alpha \, G \, b\sqrt{\rho} \qquad (12a)$$

where τ is the shear stress, G is the shear modulus, ρ is the dislocation density, and α varies from 0.2 to 0.25. Therefore ρ_s increases only at τ^2 [2]. This reveals that the actual creep rate at high stresses is much greater than that suggested by Equation (11). For example, an analysis based on the creep data of Cheng et al. [10], suggests that the high secondary creep rate observed in α Fe - 3% Si alloy would require an untenably high density of screw dislocations approaching a value of 10^{16}

per cm^2 at high stress levels. The usual level of ρ for a crept metal is about 10^{11} per cm^2. Furthermore the preferred relationship given by Equation (11) suggests that the creep rate should increase less rapidly with stress at the higher stress levels whereas the opposite is observed experimentally.

2. Climb of edge dislocations

A steady-state dislocation theory based on the climb of edge dislocations was proposed by Weertman [54,55]. Weertman assumed that during creep deformation, dislocation loops are emitted from Frank Read sources, and piled up at internal obstacles such as grain boundaries, sessile dislocations, and precipitates as shown in Figure 5. The back stress of these piled up groups will finally cancel the external stress at the sources. Hence, deformation will stop and can proceed only if a dislocation in the pile up climbs over the obstacle. The creep rate will, therefore, be proportional to the climbing rate. The climb mechanism requires that vacancies be created or destroyed at dislocations. At the tip of the pile ups, a non-vanishing hydrostatic stress $\pm \sigma_i$ may exist which exerts a force on a dislocation in a direction normal to the slip plane, and will favor climb. Vacancies will be absorbed where the stress is compressive and they will be created where the stress is tensile. This will result in a change in the vacancy concentration in the vicinity of a dislocation line and a vacancy flux is established between segments of dislocations which act as sources and segments acting as sinks. On this basis Weertman estimated that

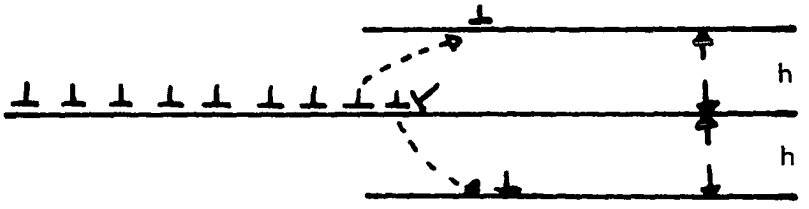

a. Climb over the sessile dislocation

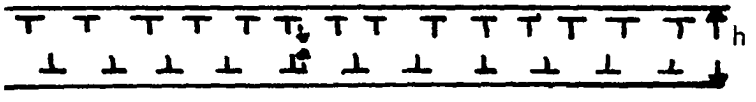

b. Annihilation of dislocations of opposite sign on parallel planes

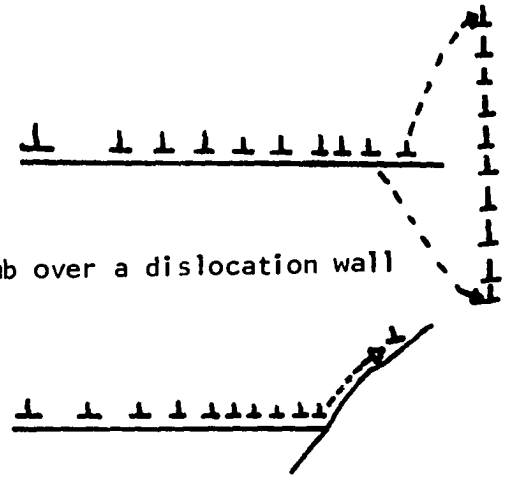

c. Climb over a dislocation wall

d. Climb over a grain boundary

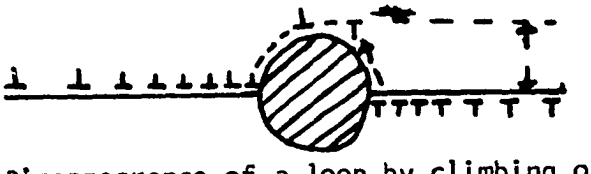

e. Disappearance of a loop by climbing over a precipitate

Figure 5. Climbing of dislocations at various obstacles during high temperature creep

$$\dot{\gamma}_s = \frac{\pi^2 \tau^2 D}{G^2 b^2} \sinh\left\{ \frac{\sqrt{3}\, \tau^{2.5} b^{1.5}}{8\, G^{1.5} N^{0.5} RT} \right\} \qquad (12b)$$

where N is the number of dislocation sources per unit volume, G is the shear modulus, τ is the shear stress, and D is the coefficient of self diffusion. At high temperatures and relatively low stresses the above equation reduces to

$$\dot{\gamma}_s = A \frac{\tau^m}{RT} e^{-\Delta H_d/RT} \qquad (13)$$

where ΔH_d is the activation energy for self diffusion, and m = 4.5. The major virtue of Weertman's theory is that it correlates quite well with most of the mechanical data on high temperature creep. It accounts for the observed apparent activation energies. However, the question of the stress dependence of the creep rate in the climbing process is more difficult to answer and depends sensitively on the finer structural details of the process [54].

F. Creep of Rutile

Rutile is the stable form of titanium dioxide. The crystal structure of TiO_2 is body centered tetragonal with oxygen ions occupying in sixfold coordination with the titanium ion at the body centered position as shown in Figure 6. Grant [20] has made a comprehensive survey of its physical properties and structure. Slip planes have been determined by several investigators. Wachtman and Maxwell [51,52] bent rutile bars at 1000°C and found slip on the (011), the (201), and

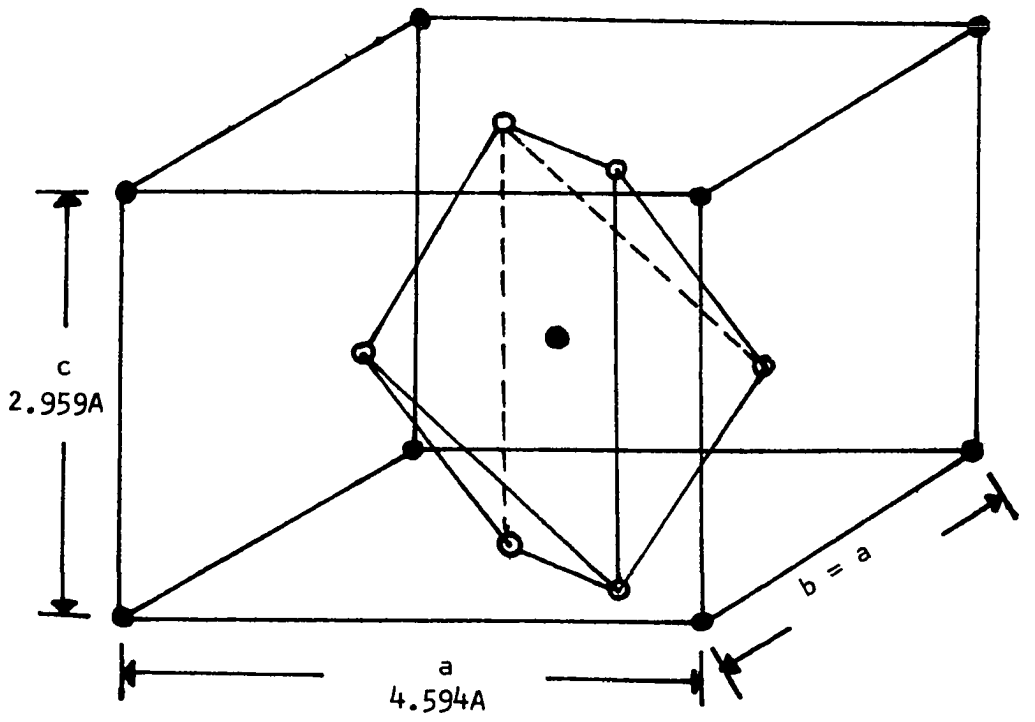

Figure 6. Unit cell of rutile (TiO_2); ● - Ti, O - O^{-2}

possibly the (110) and (101) type planes. Hirthe and Brittain [24] confirmed the (110) and (101) type planes and reported the slip direction as [001] for the (110) type plane with the corresponding Burgers vector as c [001].

Hirthe and Brittain [25] studied on the high temperature compressive creep in rutile for near stoichiometric and vacuum reduced specimens in the range 777° to 1052° C and for stresses from 2,900 psi to 13,053 psi. They reported an activation energy of 67 kcal/mole for the near stoichiometric condition and 33 kcal/mole for the highest degree of reduction. They also reported that the stress dependence of creep rate to m = 1.9, where m is the stress exponent. A model based on the intersection of piled up dislocations on a single slip system with high density polygon walls formed during creep was proposed to explain the steady state creep in rutile. They reported that the dependence of dislocation wall spacing on stress obeyed the law

$$d = K \sigma^{-2/3}$$

where

d = average spacing of walls
K = constant
σ = stress.

This is very nearly the same as the results of Servi, Norton and Grant [45] who observed that the average spacing of walls in aluminum as $d \alpha \sigma^{-0.8}$.

1. Preliminary creep experiments on rutile

High-temperature compressive creep measurements were conducted by Bell et al. [5] over the temperature range 890 to 1040°C with stresses

ranging from 5,000 psi to 12,000 psi. Prior to testing, the sample was preheated in air at 1000°C for approximately 24 hours, then lowered to the test temperature for two hours to stabilize the system. This preheat was utilized to insure near stoichiometry and essentially constant thermal history. A typical creep curve at a constant stress of 10,000 psi and temperature 1020°C is shown in Figure 7.

Comparison of the results of incremental stress tests and secondary creep rates of specimens crept at the same temperature but different stresses indicates that the creep rate of rutile varies with stress in a power relation:

$$\dot{\epsilon} = A\,\sigma^{m} \tag{15}$$

with m = 1.8. This value agrees closely with the value previously reported by Hirth and Brittain [25]. The temperature dependence of rutile was investigated by testing specimens at the same stress but at different temperatures by comparing their secondary creep rates since

$$\dot{\epsilon} = A'\,\sigma^{m}\,e^{-\Delta H_c/RT} \tag{16}$$

where

ΔH_c = apparent activation energy for creep

R = gas constant

T = creep temperature in °K.

This procedure gave an activation energy for creep, ΔH_c, of 66 kcal/mole, a value which agrees quite well with that of ΔH_c = 67 kcal/mole, reported by Hirthe and Brittain [25]. This would appear to indicate that the rate

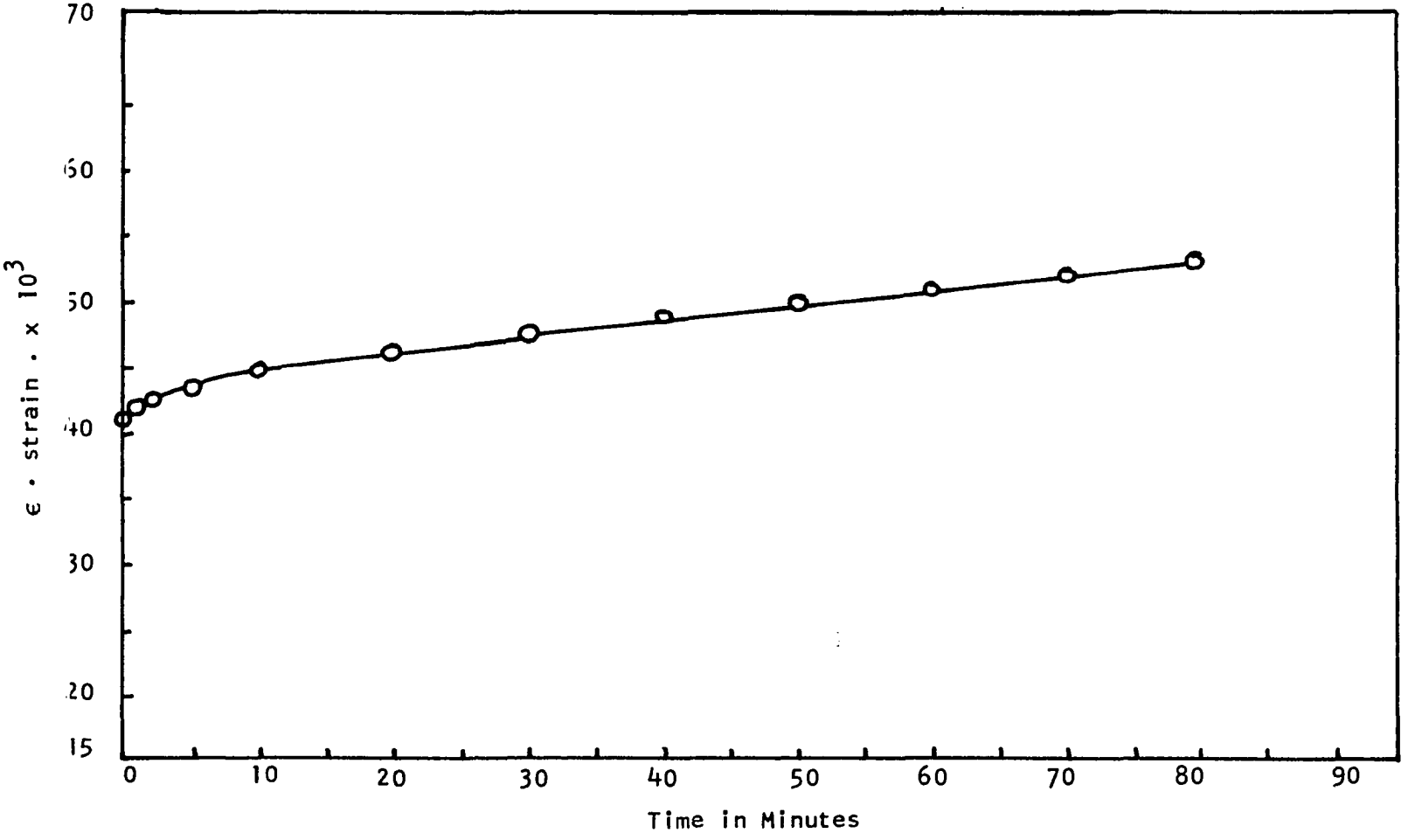

Figure 7. Creep curve at T = 1020°C, and σ_o = 10,000 psi

controlling process for creep involves the diffusion of O^{-2} ions, for Haul and Just cited in [25] have reported a 72 kcal/mole activation energy for diffusion of O^{-2} ions, and Whitmore and Kawai [58] have reported that the activation energy for sintering is 70 kcal/mole, which they also attribute O^{-2} diffusion. In view of the above results the creep mechanism in rutile would appear to be due to the climb of edge dislocations.

The temperature dependence of creep in general was discussed in Section C of Chapter II. It was confirmed by Bell, Krishnamachari and Jones [5] that the functional relationship of Equation (9) holds true for rutil As shown in Figure 8, the juxtaposition of the curves over the ent' range of creep strains also indicates that the activation energy for creep is independent of strain (i.e., significant substructural details).

Under the conditions where the stress is increased at the same value of θ_c for creep at three different temperatures as in Figure 9, excellent agreement was obtained with the values predicted by Equation (9), even though the function f varies with stress. By differentiating Equation (9) with respect to time, the creep rate is given by

$$\dot{\epsilon} = \frac{d\epsilon}{dt} = f' \left(t\, e^{-\Delta H_c/RT}\right) \cdot e^{-\Delta H_c/RT} \qquad (17)$$

where σ is constant, $f' = \frac{\partial f}{\partial \theta_c}$, and $\theta_c = t\, e^{-\Delta H_c/RT}$

From this, one can conclude that the instantaneous creep substructure, at a given stress, must vary with $f'(\theta_c)$ and therefore depends on θ_c and σ independent of temperature. Data such as that in Figure 9 are

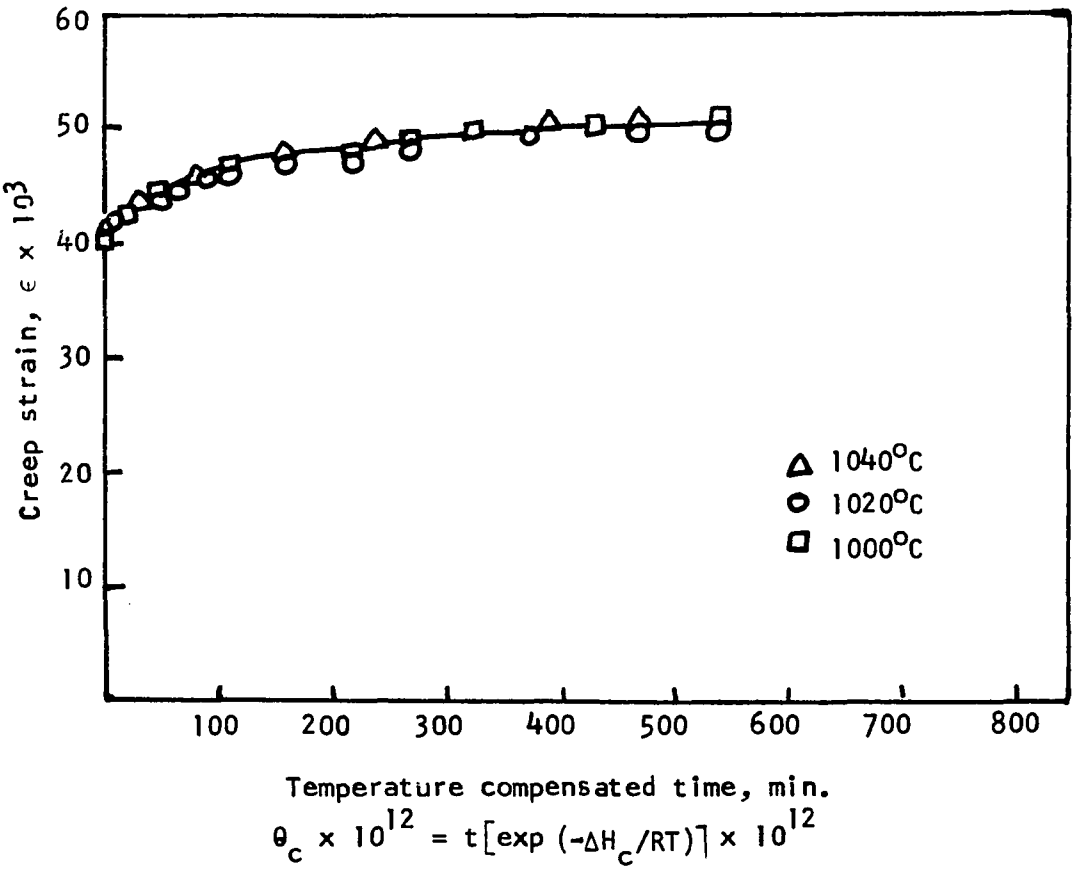

Figure 8. Creep curve for rutile under a constant stress of 10,000 psi as a function of θ_c

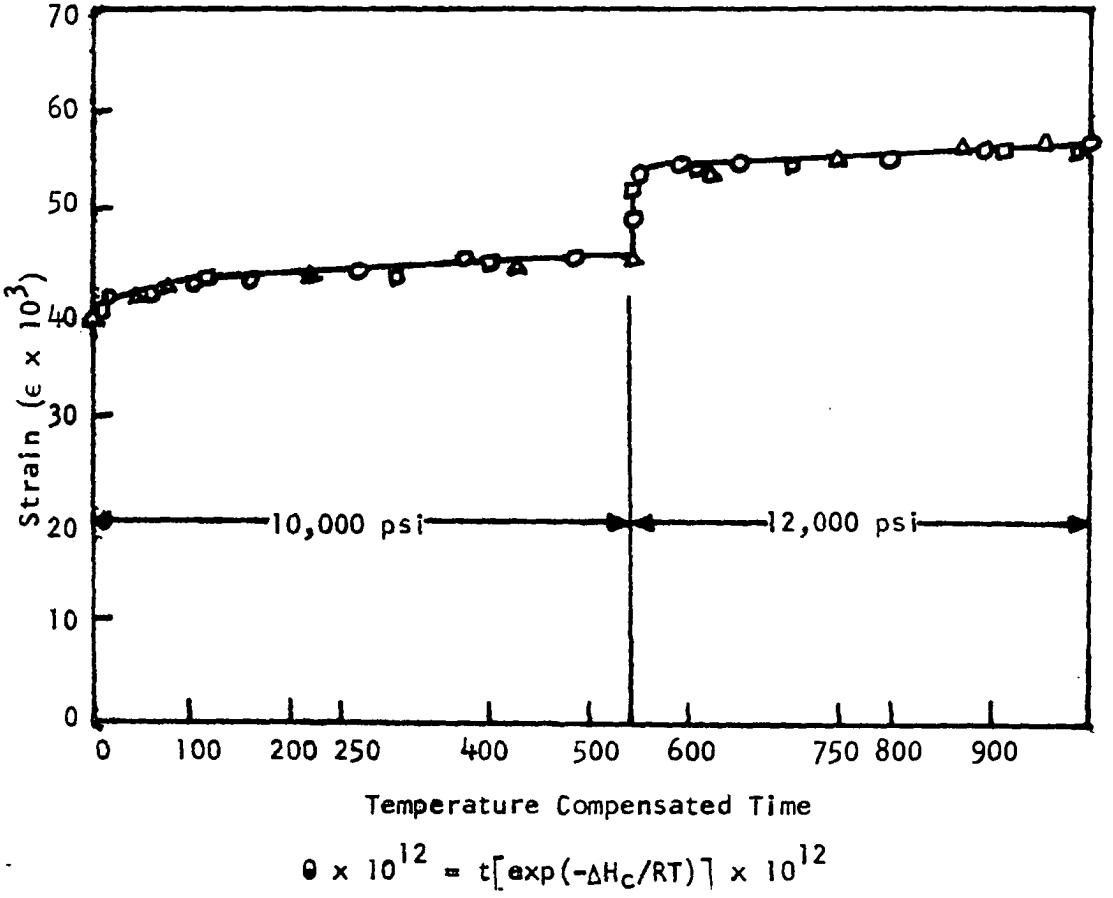

Figure 9. Validity of the temperature - compensated time concept for an increase in creep stress

extremely sensitive to substructural changes and strongly suggest the identity of the creep resistant substructures at equivalent values of θ_c.

The creep of single crystals of rutile was also studied by Farb et al. [15], as a function of stress, temperature, ambient atmosphere, and impurity. For constant ambient and impurity conditions in the range 1100^{o} to 1230^{o}C and stress ranging 5,546 to 10,324 psi, the steady state deformation rate fitted well to

$$\dot{\epsilon} = A \exp\left(B\sigma - \frac{\Delta H}{RT}\right) \tag{18}$$

under conditions of constant or decreasing temperature. The coefficient A ranged between 10^{10} to 10^{19} for undoped specimens in N_2, decreased by a factor of 10^3 in O_2, and fell to 10^0 and 10^{11} for doping with Fe and Al, in O_2, respectively. The quantity B, ranged 1.0 - 2.2 in N_2, and 0.7 - 1.4 in O_2, while the activation energy ΔH ranged from 129 to 155 kcal/mole in N_2, 92 to 152.5 kcal/mole in O_2, 53 and 133 kcal/mole for doping with Fe and Al in O_2, respectively. ΔH increased abruptly by 46 kcal/mole at a stress between 5,546 and 6,399 psi with accompanying changes in A and B. They also observed a higher creep rate for the specimens cut from the center of the rutile boule, by as much as a factor of two, than those cut from near the surface of the boule. Spectrographic analysis indicated a somewhat lower impurity concentration for the specimens near the center of the boule. Bell et al. [6] found no such variation of creep rate for the specimens cut from the center and from near the surface of the boule. Farb et al. [15] concluded that the large

variation in the creep constants ΔH, A, and B indicates that the steady state creep of rutile is not controlled by a single simple mechanism. The variation in activation energies may be the competition of two rate limiting mechanisms, (1) the climb of jogs on screw dislocations, and (2) the pinning of dislocations by impurity oxygen vacancy complexes.

Creep results of Farb et al. do not agree either with the results of Hirthe and Brittain [25], or Bell et al. [6].

G. Effect of Intermittent Stress Treatment on Creep Deformation Behavior

Materials for specific industrial applications are usually evaluated on the basis of simple laboratory type tests. But in reality these materials function under service conditions far different from those under which they were evaluated in the laboratory. For example, materials for high temperature service as gas turbine buckets or nuclear reactor pressure vessels are selected on the basis of creep and stress rupture tests in which the elongation and rupture time are measured at constant temperature and stress. In service, however, the turbine bucket or the pressure vessel are likely to be subjected to heat shock, vibration, periodic removal of load, temperature, or both. Therefore, it is better to expand the evaluation tests of materials of interest for various applications to include more realistic conditions likely to be encountered in their service applications. One step in this direction is to include the effect of intermittent loading on the creep behavior of materials.

The important metallurgical and mechanical factors which must be

considered when the component design involves change of stress are:

1. anelastic effects on the creep flow
2. change in strain hardening
3. changes in microstructure [38].

1. Anelastic effects on creep flow

If the stress is removed following previous extension in creep, a specimen will undergo a time dependent contraction. Chalmers [9] conducted creep recovery experiments on tin at room temperature and extremely small strains. If the stress is so low (85 psi) that the creep gradually fades out with time (transient creep), then on unloading, the strain is totally recovered at a rate nearly identical with that of previous extension. Ke [27] has reported similar anelastic behavior in polycrystalline aluminum wires subjected to very small creep strains in tortion.

Zener [62] has discussed the physical origins of such anelastic effects. He pointed out that the anelasticity observed in creep can be primarily related to stress relaxation across inhomogeneous regions in the material. He further suggested that micro-cracks may form in these locations. It may be possible that many repetitions of a load cycle leading to anelastic extension and recovery could cause propagation of these cracks and thereby accelerate fracture.

2. Change in strain hardening

Strain hardening loss or recovery can occur during periods of reduced stress. Lequear and Lubahn [33] have demonstrated this effect in

a Cr-Mo-V steel, subjected to creep at 538°C. The test temperature and creep times were such that no tempering would be expected during the test. Specimens were unloaded after a given creep strain and rested at zero stress at 538°C for several time periods and then reloaded with the initial stress. The strain rate after interruption is higher than that existing previously, indicating that a loss of strain hardening occurred.

Lubahn [35] discusses another phenomenon which may occur when the load is removed and then restored. Room temperature creep of copper was interrupted by a period of no load and the test was then resumed at the initial load. He noted that the creep rate following the reapplication of the load is initially high and gradually falls to a value nearly equal to that established before interruption indicating a transient softening. Recovery of creep resistant substructure under reduced stress treatment was studied by Kennedy [29], Bull [7], Dorn and his co-workers [36,44] and Bell et al. [6]; in lead aluminum and rutile respectively. Details of their work are discussed in the next few sections.

3. Changes in microstructure

Changes in microstructure include overaging, aging and recrystallization. Many materials gain their strength and creep resistance from the presence of finely dispersed precipitated particles. Any tendency to alter the number, size, and shape of the precipitate may alter creep, stress-rupture, and fatigue characteristics. If the particles agglomerate and their size becomes larger than an optimum value, the hardness of the material and its creep resistance may decrease. This condition is called

overaging. In testing the aluminum alloy 24S - T_3, Guarnieri [21] found that the intermittent stress treatment accelerated the overaging. This may be due to the greater number of deformation sites available for agglomeration.

It has also been observed that aging may be promoted by changing load conditions during creep [21]. In some cases aging may be beneficial, owing to increased creep resistance. In other cases ductility may be sufficiently reduced to shorten rupture life.

Recrystallization may also accelerate the creep due to the relief of internal stress. Cycling the load has a tendency to accelerate recrystallization. Guarnieri [21] observed this tendency in FS-1H magnesium alloy. For approximately the same total elapsed time at temperature, and approximately the same amount of total deformation, the intermittently loaded specimen was in a more stress relieved and recrystallized condition than the constantly loaded one.

Ordering increases creep resistance. For example for β-brass tested in creep under a tensile stress of 360 psi, Martin et al. [39] found a sharp increase in the creep rate at $T_c = 470^{\circ}C$. This increase coincides with an order-disorder transformation which occurred in this material at the transition temperature $T_c = 470^{\circ}C$. Just below the transition temperature T_c, inverse primary creep (opposite to decrease in creep rate) was observed. When the stress was removed in the primary region, reverse recovery (hardness back to the original condition) occurred. Removal of stress restored order by diffusion, and strengthening took place.

H. Creep Recovery

1. General discussion on recovery

When a material is plastically deformed by creep or cold working a certain fraction of the mechanical energy which is expended during the deformation process is stored in the material in the form of various types of imperfections. The energy thus stored in the material renders it thermodynamically unstable with respect to the unstrained, well annealed condition. If the cold worked material is heated, atomic mobility would take place under an applied stress, and there would be a tendency for the deformed material to return again to the lower energy, annealed state. Recovery can be considered to be any modification of properties or structure which is brought about by annealing plastically deformed materials, but without the formation of new strain free recrystallized grains. Recrystallization is defined as the appearance of comparitively strain free grains which are separated from the deformed matrix or other recrystallized grains by high angle grain boundaries.

Vandermeer and Gordon [50] studied the influence of recovery on recrystallization in zone refined aluminum containing a small quantity of copper. They found that the increase in impurity content would favor recovery over recrystallization. The activation energy for recovery was increased from 13 kcal/mole to 19 kcal/mole as the copper content was raised from 0 to 0.0068 atomic percent. Over the same composition range the activation energy for recrystallization increased from 15 kcal/mole to 30 kcal/mole. So the rate of recrystallization decreases much faster than that of recovery as the copper content is raised. Thus recovery

was favored over recrystallization as the copper content increased.

Gay et al. [17] found that recovery is associated with the rearrangement of dislocations in the subgrain boundary regions and with possible movement of dislocations from the subgrain boundary. Small increases in subgrain size were detected by Perryman [43] during the recovery annealing of deformed aluminum at temperatures near the recrystallization temperature. Subgrain growth must, therefore, be listed as a possible recovery mechanism. Weissmann [56] investigated the kinetics and orientation of subgrain growth in polycrystalline aluminum cold rolled 81.7%. He noted that certain subgrains highly misoriented with respect to the neighboring subgrains grew rapidly. Weissmann et al. [57] have noticed the growth of subgrains in cold worked aluminum when annealed. This growth occurred by a gradual disappearance of the subgrains.

Hu [26] who has studied and observed this phenomenon in 3% silicon iron single crystals, cold rolled 70%, termed it subgrain coalescence and explained coalescence on the basis of subgrain rotation. The coalescence of subgrains through the gradual disappearance of their common boundary may be explained by the movement of dislocations from the disappearing boundary into the connecting boundaries around the subgrains. Such a process will probably involve dislocation climb along the disappearing boundary and rotation of the lattice orientation requiring the movement of some of the atoms around the subgrains. The process of subgrain rotation was thoroughly analyzed by Li [34]. He concluded that the recovery process in silicon iron single crystals can be divided into

three stages: (1) the annealing out of vacancies; (2) the annihilation and rearrangement of dislocations; (3) the formation and growth of subgrains by coalescence.

Based on photo micrographs of bent and annealed silicon iron crystals, Hibbard [22] postulated that dislocations migrate down the polygon boundary to a higher angle subboundary which might eventually remove the polygon subboundary and result in the growth of polygon width.

Smith and Dillamore [48] have studied the subgrain growth in 70% cold-rolled high purity iron. Detailed electron-microscope study of the kinetics of the subgrain growth revealed that the subgrain growth was sensitive to orientation, being greatest in the (110) $[\bar{1}10]$ orientation and least in the (001) $[\bar{1}10]$ orientation. Based on the coalescence theory of subgrain growth, they estimated the time required to produce a specific increase in subgrain size. It differed several orders of magnitude from the measured value. An alternative view of subgrain growth analogous to ordinary grain growth was found to explain the orientation dependence of subgrain growth.

2. Recovery of creep-resistant substructure in aluminum

Recovery of the creep resistance of 99.99 percent pure aluminum was studied by Ludemann et al. [36] at temperatures 540, 573, 600, and 611°K. Polycrystalline specimens crept to a strain of 5.5 percent were allowed to recover for periods of from 1 min to 16 days. Increased creep rates upon reapplication of the 950 psi evidenced softening of the material. The activation energy for the recovery process was found to be

64 kcal/mole.

Raymond and Dorn [44] analyzed the recovery of creep resistant substructure of high purity aluminum under reduced stresses. Analysis of the kinetics of the recovery as a function of the temperature gave a stress sensitive activation energy that decreased as the reduced stress was increased from a value of 64 kcal/mole at 10 psi to 37 kcal/mole at 750 psi. They suggested that the major factor responsible for the recovery under reduced stresses is the migration of subboundaries. They also suggested that the applied stress aids the thermal activation of the subboundary motion and that the activation energy for motion at zero stress is greater than that for self diffusion due to the effect of impurity atom pinning.

In Al - 1.8 a/o Mg solid solution, Bell [3] found no recovery, a phenomenon which he attributed to subgrain boundary pinning by the Mg atoms.

3. Recovery of creep-resistant substructure in lead under zero stress

The influence of reduced load on the creep behavior of lead was first investigated by Kennedy [29]. Room temperature creep was interrupted by load removal and the specimens held at various temperatures for 30 min. The room temperature creep was then resumed at the prior stress. He observed that the creep was accelerated after reloading. Tests were also reported by Kennedy [28] in which room temperature creep was interrupted by a 53 min. rest at no load following different amounts of prior creep. According to Kennedy the creep rate after interruption was raised and this effect decreased with increasing

amounts of prior creep strain.

Kennedy [30] was the first one to determine the activation energy for the recovery under zero stress in lead. He obtained an activation energy of 19.8 kcal/mole for the recovery under zero stress. He suggested that the recovery process provides the nuclei for recrystallization and the activation energy for the growth of new material was found to be 31 kcal/mole.

Recently Bull [7] has conducted constant stress, constant temperature creep tests on 99.99% pure lead. He obtained an activation energy for creep of 23.5 kcal/mole. He obtained an activation energy of 24 kcal/mole for the recovery of creep resistant substructure under zero stress. He reported that the activation energy for recovery in his study was 2 percent of the value for grain boundary migration reported by Gifkins [18]. Subsequent optical microscopic work by Bell [4] has revealed no evidence of grain boundary migration, however.

4. Recovery of creep resistant substructure in rutile under zero reduced stress

Bell, Krishnamachari and Jones studied the recovery of creep resistant substructure in rutile under zero reduced stress [6]. Compressive creep specimens were crept under a stress of 10,000 psi to a strain early in the secondary stage of creep and then allowed to recover for varying periods of time under a residual stress of 500 psi. Recovery was detected by the increased amount of creep strain which occurred upon reapplication of the 10,000 psi stress. They obtained an apparent

activation energy of 135 kcal/mole for the recovery of creep resistant substructure under zero reduced stress. They suggested that the primary recovery mechanism involves the sweeping out of dislocation barriers within the material by the migration of dislocation walls or subgrain boundaries.

III. EXPERIMENTAL APPARATUS

The creep testing apparatus used in this investigation consisted of a massive steel loading frame. Loads were applied by a lever system to a vertically centered alumina loading ram. Alumina was used because it is harder and the melting temperature is higher than rutile. So at the testing temperature 1100°C, alumina is stronger than rutile. Alumina discs of 3/4 in. diameter and 1/2 in. thickness were used to ease sample loading and to protect the loading rams. A split furnace was used in which each half could be rolled away from the specimen to permit pre and post-test handling. The furnace contained four bayonet type silicon carbide heating elements. The temperature was proportionately controlled within $\pm$ 2°C. The experimental set up is shown in Figures 10 and 11.

The deformation of the specimen was recorded continuously using a linear variable differential transformer (LVDT) and was autographically recorded. The LVDT read-out has different ranges of span and the deformation could be measured with an accuracy up to one hundredth of a mil. The LVDT was calibrated by using a micrometer head for various ranges of span in the differential transformer read-out. Load was applied by means of an hydraulic jack fixed to the "A" frame. The upper loading lever was lowered slowly by means of this jack in order to eliminate the possibility of impact loading and to insure reproducibility in the rate of application. The upper and lower loading rams were leveled from time to time by using a head gage whose span can be measured by means of a micrometer. The leveling of the alumina rams eliminated the possibility of an uneven load

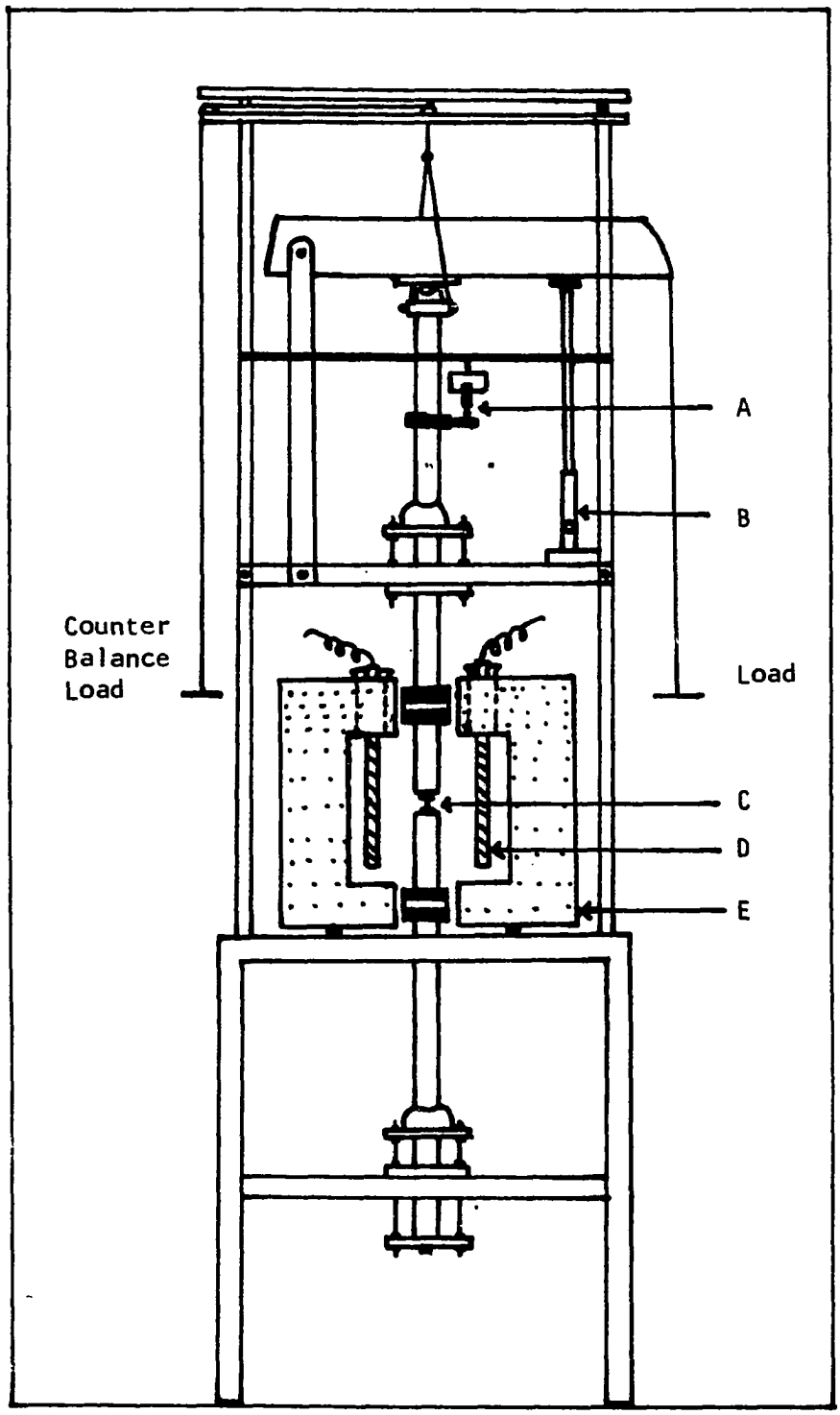

Figure 10. Creep testing machine. A. LVDT B. Hydraulic jack, C. Specimen D. Heating element E. Insulation

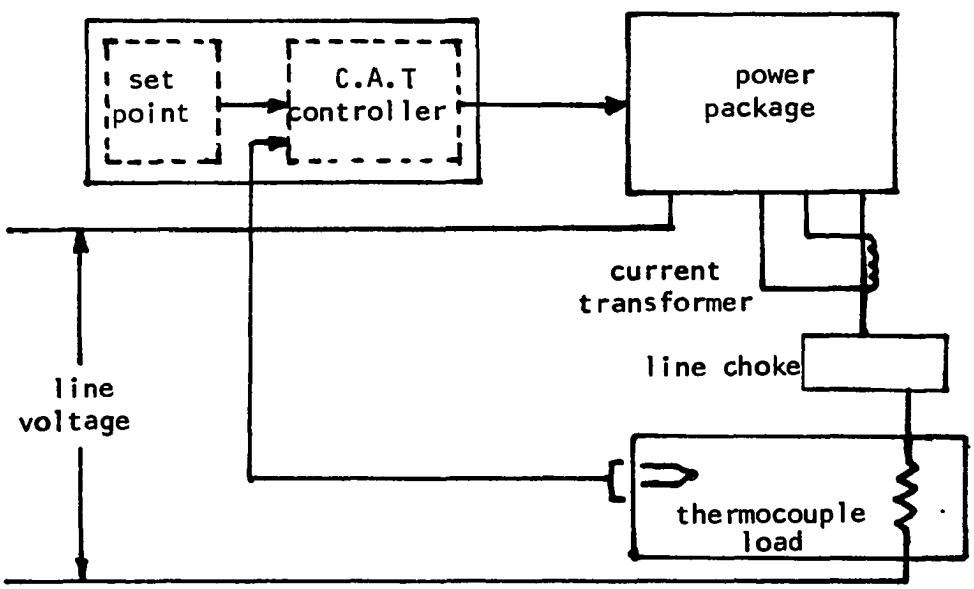

Figure 11. Current adjusting type control system

distribution on the test specimen. Thermal expansion of the steel loading ram was reduced by cooling the loading rams. In this manner, adequate precautions were taken to minimize all probable sources of error in the creep testing.

IV. EXPERIMENTAL PROCEDURE

A. Sample Preparation

A 3/4-in. diameter, 5-in. long boule of undoped synthetic rutile was obtained from the Linde Division of Union Carbide Corporation. The analysis of impurities supplied by the manufacturer is given in Table 1.

Table 1. Impurity content of rutile boule

Element	Amount	Element	Amount
Al	3 - 5 ppm	Ni	[a]
As	5 - 10 ppm	Nb	[a]
Cr	[a]	Sb	3 - 5 ppm
Cu	[a]	Si	5 - 10 ppm
Fe	15 - 25 ppm	Sn	3 - 5 ppm
Mn	[a]	V	3 - 5 ppm

[a] Trace elements.

The growth axis orientation of the boule was determined by a Laue back reflection X-ray technique. After orientation, the boule was cut using a Di-Met cutoff machine to obtain 0.1 x 0.1 x 0.2 in. rectangular parallelopipeds (Figure 12), with an optimum height/width ratio of 2:1 [1] (Ashbee and Smallman reported that with shorter heights the flow stress began to increase rapidly because of end effects at the surfaces in contact with the compression plungers; with longer heights inhomogeneous deformation occurred. Compression tests on crystals of various

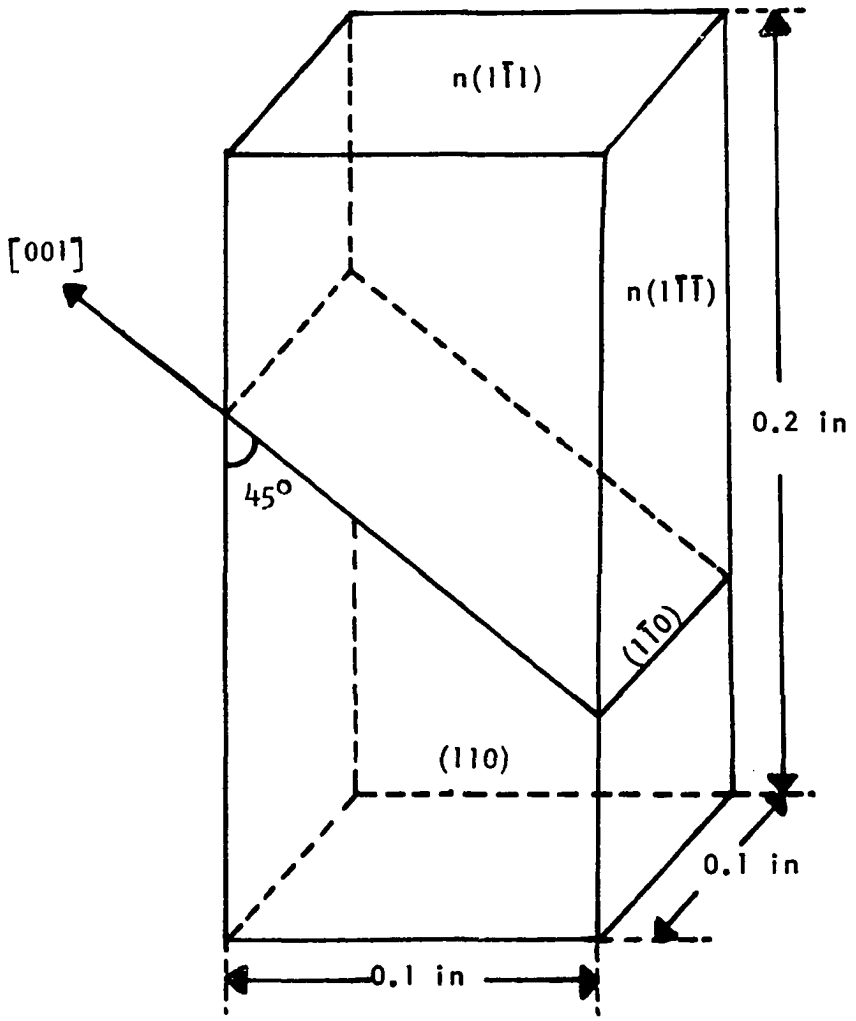

Figure 12. Orientation and approximate size of rutile single crystal compressive creep specimen

heights showed that the optimum height/width ratio was 2:1.) All cutting was done with 600-grit diamond wheels at a very slow feed rate with the cutting wheel dressed down at frequent intervals. This was followed by light mechanical polishing on dry 600-grit SiC sand papers to obtain final specimen sizing. Polished samples were checked for orientation on a random basis using Laue back reflection X-ray technique. The $(1\bar{1}0)$ [001] slip system is inclined at 45^{o} to the long axis as shown in Figure 12.

After cutting and lapping, the specimens were chemically polished to remove any surface deformation zone which might affect the subsequent test results. All specimens were chemically polished prior to creep testing by immersing them with agitation in a fused KOH bath at $400^{o}C$ for 20 minutes. The amount of material removed was about 4-5 mills on the (110) surface and 6-8 mills on the {111} type surfaces. A surface film remained in many cases and could be removed by placing the samples in hot concentrated HCl. The samples were then rinsed first in methnol then in ether.

Etch pit work was carried out to study the dislocation patterns and densities at various stages of $\sigma_o \rightarrow \sigma_r \rightarrow \sigma_o$ tests. An etch pit technique utilizing an immersion of crept rutile specimens in boiling sulphuric acid for 20 minutes yielded etch pits which were satisfactory for optical metallographic examination.

B. Experimental Procedure and Results

Rutile specimens were crept to the same creep strain, ϵ_c, prior to the reduced stress recovery treatment, to insure that they had the same

creep resistant substructure. With this condition of identical creep resistant substructure, the creep stress was reduced from σ_o to a reduced stress σ_r where $\sigma_r < \sigma_o$, for various time periods at constant temperature, following which the original stress σ_o was reapplied. Recovery was detected because after the specimen had been subjected to the reduced stress treatment, the creep strain, ϵ_R, lay between that of the original annealed material (completely recovered), ϵ_c, and that of the material not subjected to a recovery treatment, ϵ_u, when the strains were plotted on the same co-ordinate axes. This permitted the determination of the fractional recovery index, n, from

$$n = \frac{\epsilon_R - \epsilon_u}{\epsilon_c - \epsilon_u} \quad . \tag{19}$$

The recovery parameter n has a value of 0 when no recovery takes place and a value 1 if complete recovery occurs. In all the tests, n had a value in the range $0 < n < 1$. A schematic illustration of a typical creep recovery experiment is shown in Figure 13. Following a recovery period, t_r, at a reduced stress, σ_r, the initial creep stress σ_o was reapplied, and the creep strain ϵ_R occurred. If no recovery had occurred during the reduced stress treatment, the creep strain ϵ_u would have been obtained. On the other hand, if the recovery had been complete, the creep strain ϵ_c would have been obtained. Schematic illustrations of a typical creep recovery experiment at a reduced stress of 5,000 psi and temperature 1020°C, are shown in Figures 14 and 15. In calculating the value of the recovery parameter, n, it appeared to be virtually independent of the position along the creep curve at which it was calculated. Nevertheless,

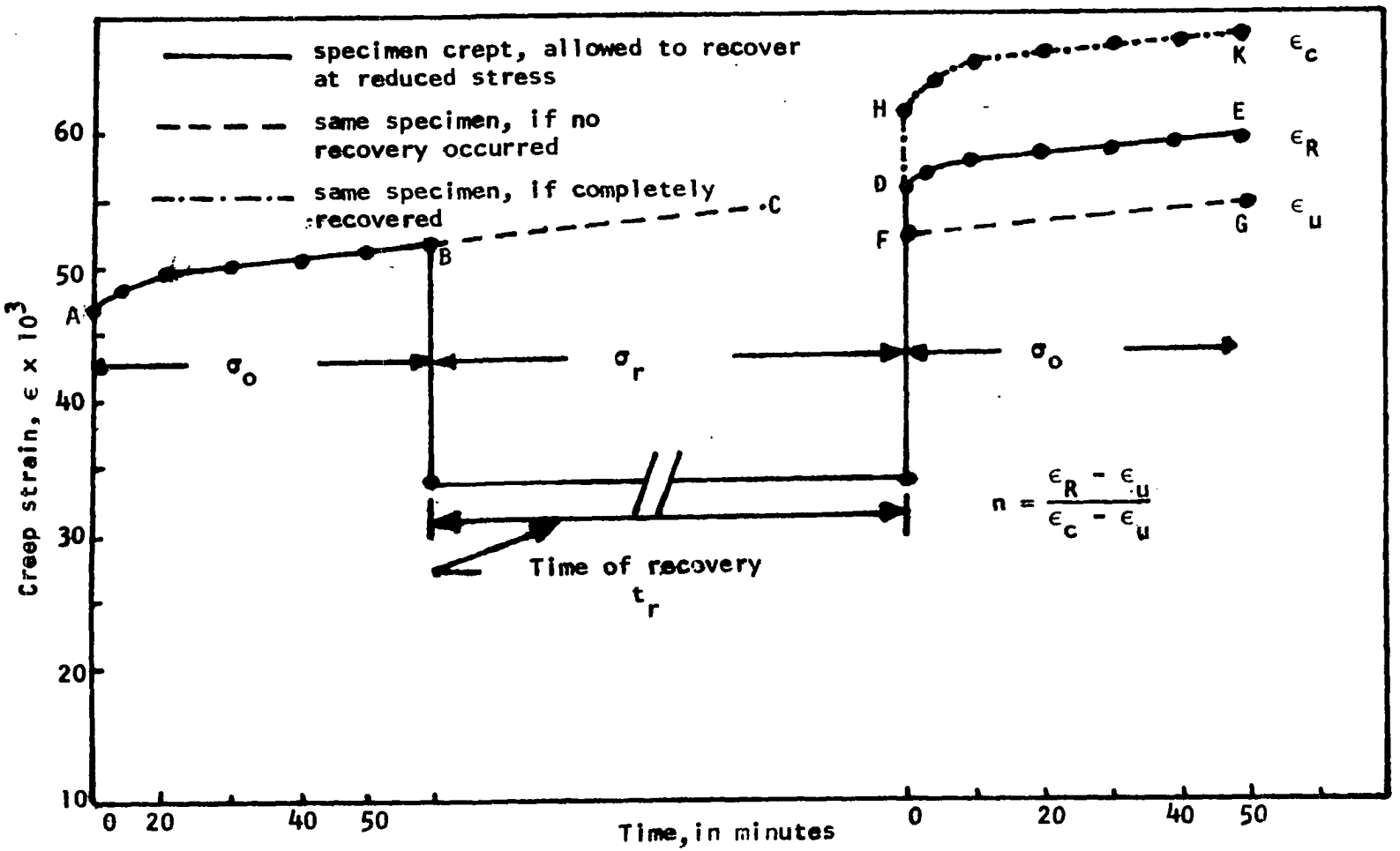

Figure 13. Schematic illustration of a thermal creep recovery experiment and creep recovery parameter determination

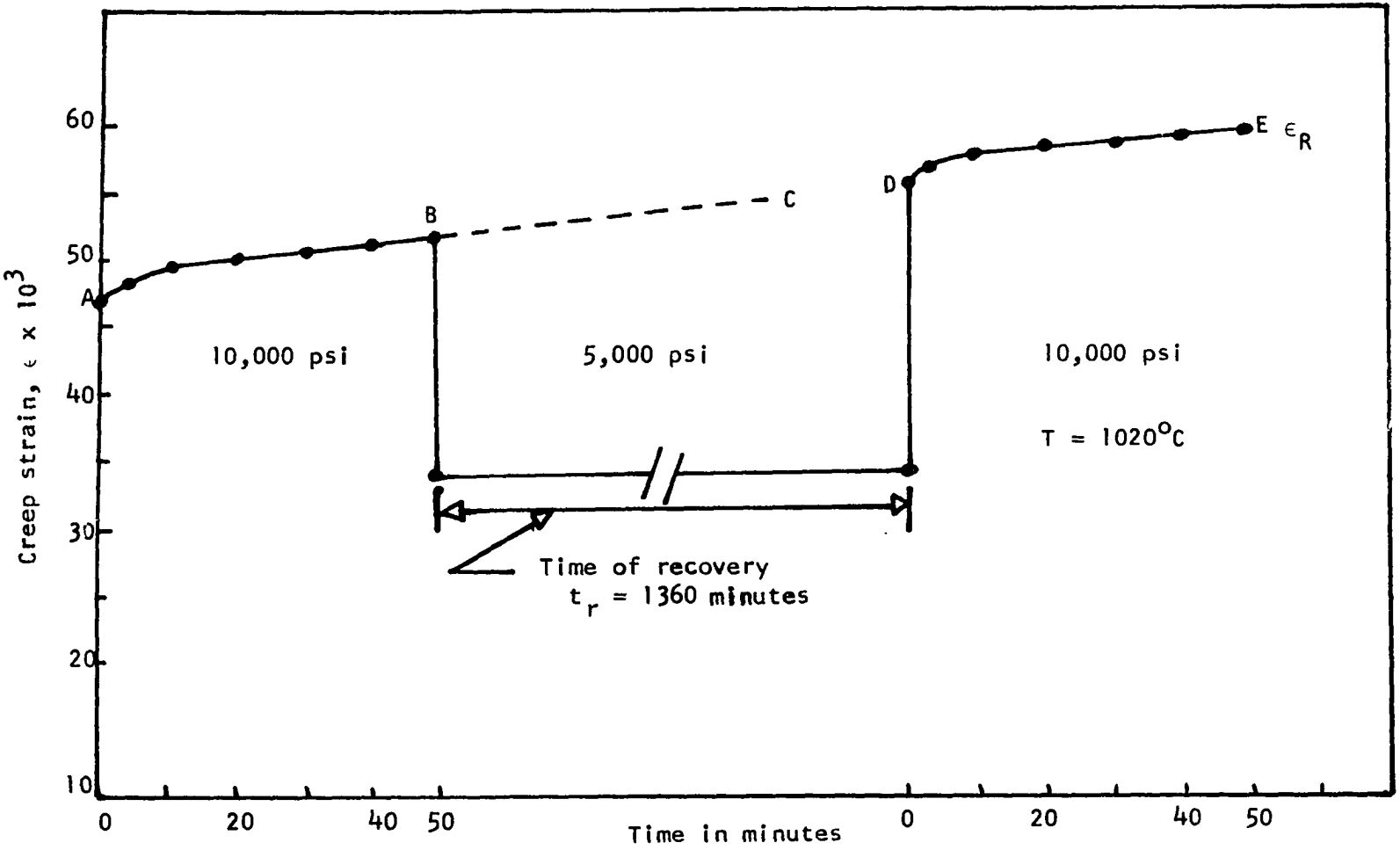

Figure 14. Schematic illustration of a typical creep recovery experiment at a reduced stress of 5,000 psi, and 1020°C

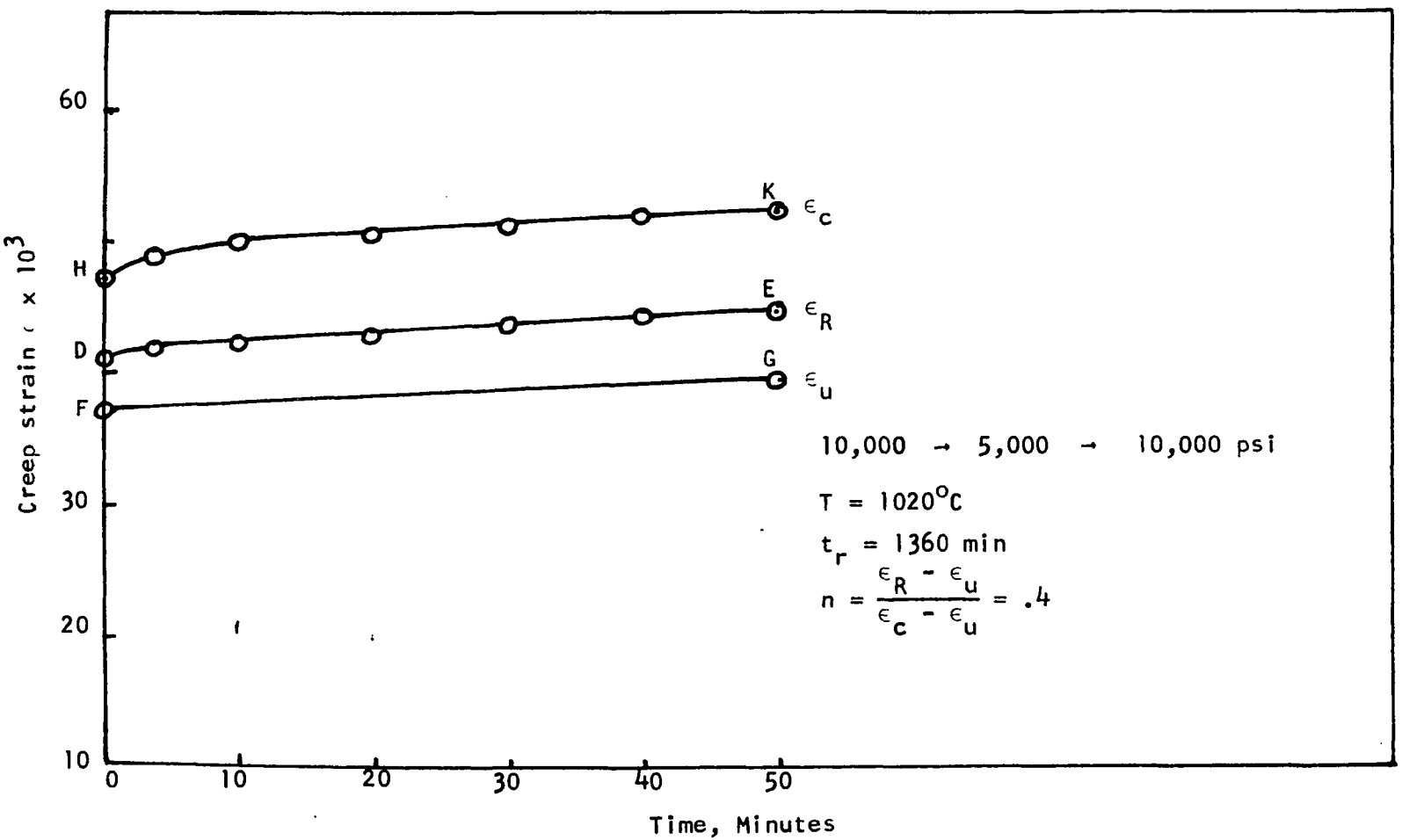

Figure 15. Juxtaposition of the various regions of Figure 14 on a common strain and time axis

care was taken throughout to evaluate n at the same temperature compensated time after reapplication of the original stress in comparing the n values of various test series.

When n is plotted against t_r, the recovery time, on log-log plot, a straight line was obtained as shown in Figures 16, 17, and 18, for reduced stresses of 2,500, 5,000, and 7,500 psi. This made it possible to compute an activation energy ΔH_r for the recovery of creep resistant substructure at a reduced stress σ_r. The recovery rate upon removal of the creep stress $\sigma_o \rightarrow \sigma_r$ can be expressed in terms of a generalized Arrhenius relationship:

$$-\frac{dS}{dt_r} = f\ (S,T)\ e^{-\Delta H_r(S,T)/RT} \qquad (20)$$

S = a substructure parameter;

f = recovery per unit time per unit probability of thermal fluctuation;

ΔH_r = the energy per mole which must be supplied by thermal fluctuations to thermally activate the unit recovery process,

T = temperature in ^oK

R = gas constant.

If it is assumed, a priori, that the activation energy for creep recovery is not a function of substructural details and test temperature, and if the reasonable assumption that f(S,T) is practically independent of T, then the apparent activation energy can be determined. Under these conditions identical substructural states are obtained by recovering for appropriate times t_{r_1} and t_{r_2}, at two different temperatures T_1 and T_2

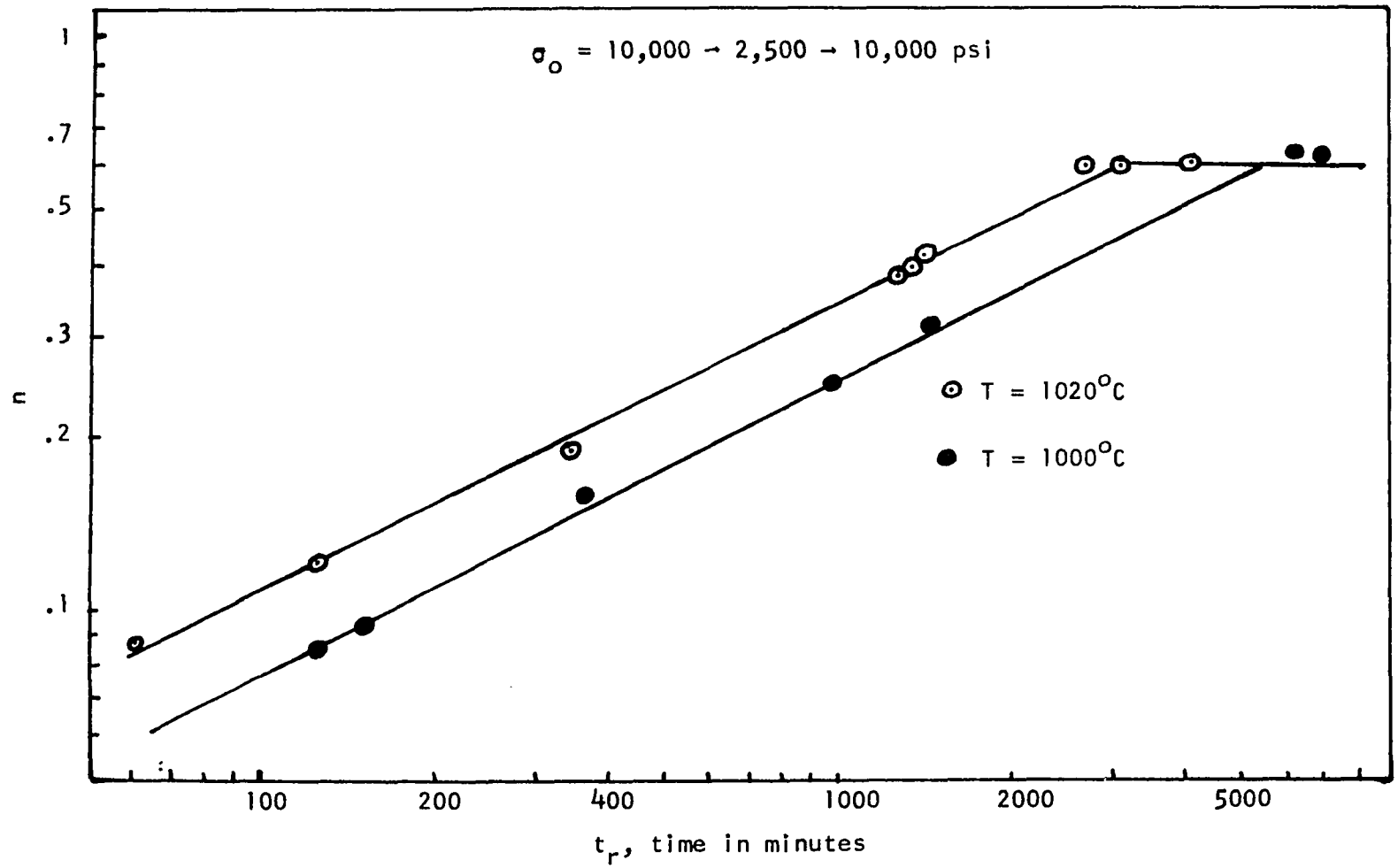

Figure 16. Fractional recovery index as a function of time at a reduced stress of 2,500 psi

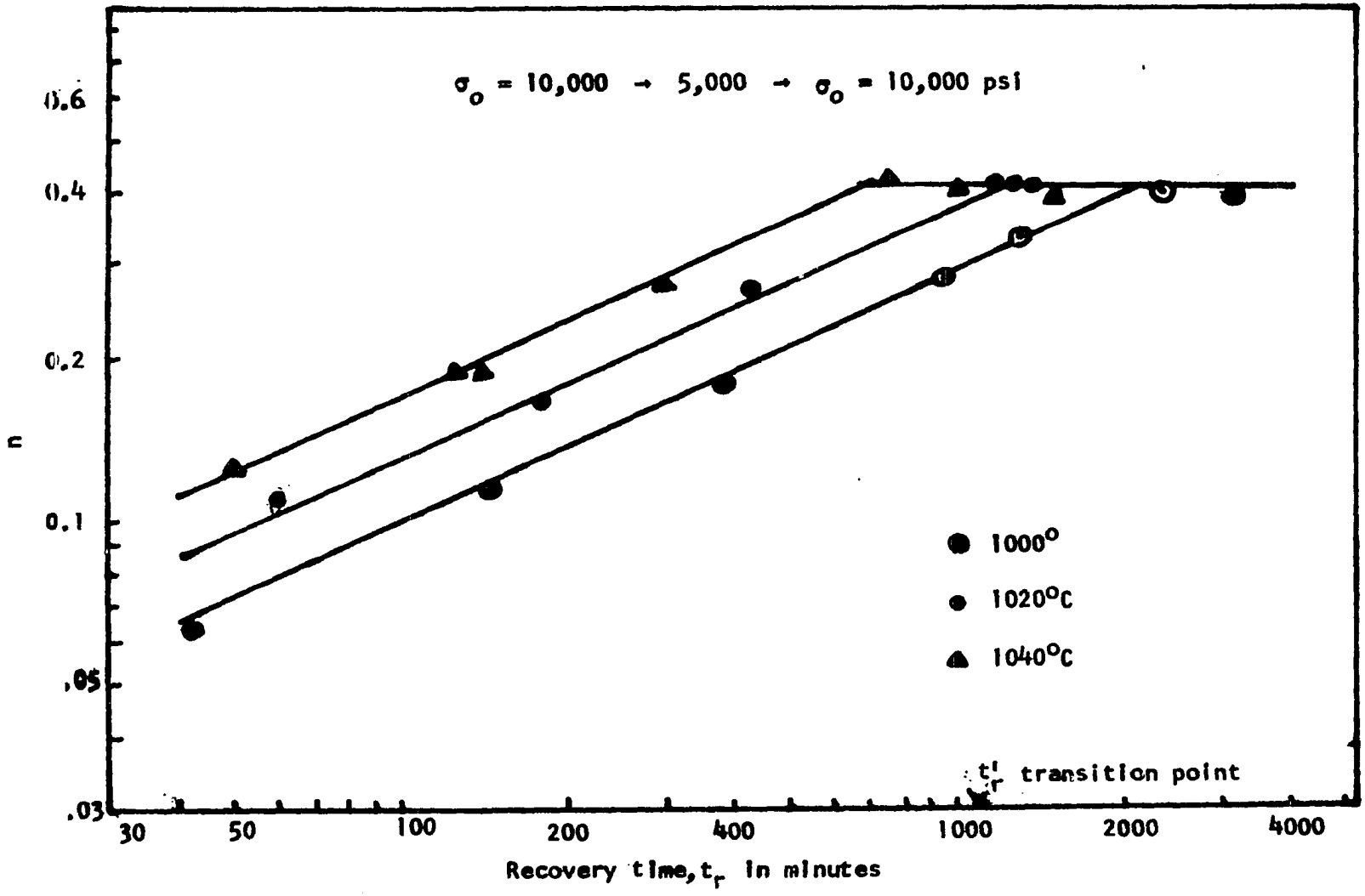

Figure 17. Fractional recovery index as a function of time at a reduced stress of 5,000 psi

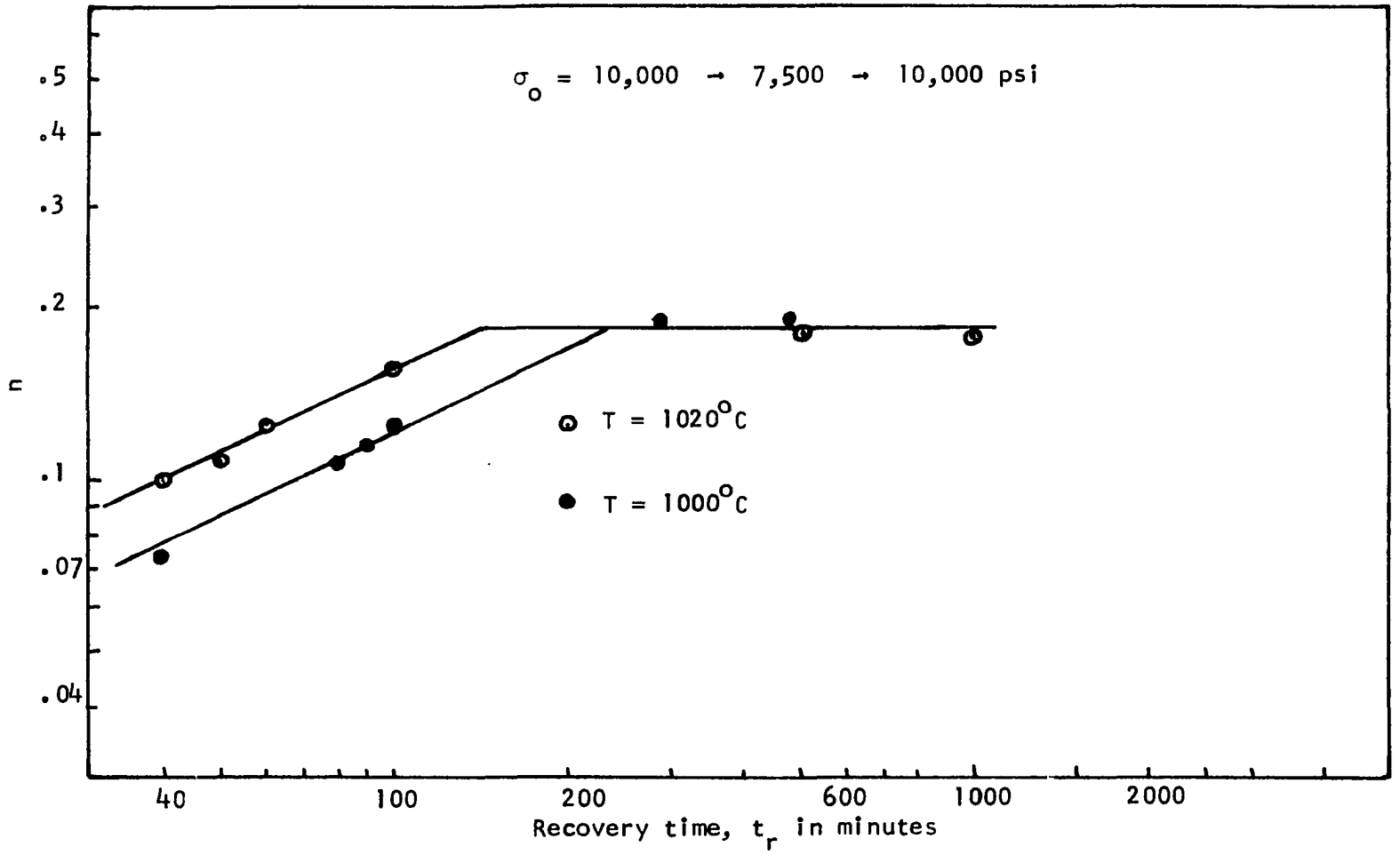

Figure 18. Fractional recovery index as a function of time at a reduced stress of 7,500 psi

to yield the same degree of recovery (same n). The recovery parameter is then a unique function of structure and for a given amount of recovery

$$t_{r_1} e^{-\Delta H_r/RT_1} = t_{r_2} e^{-\Delta H_r/RT_2} \tag{21}$$

Solving for ΔH_r, it is given by

$$\Delta H_r = \frac{R \ln[t_{r_1}/t_{r_2}]}{\left(\frac{1}{T_1} - \frac{1}{T_2}\right)} \tag{22}$$

For a given amount of recovery the ratio of times t_{r_1}/t_{r_2} at two different temperatures can be obtained from the log-log plots of n vs t_r, such as Figure 16. In this manner the activation energy for recovery of creep resistant substructure were obtained at three different stresses. The mean value of the activation energy for recovery at the different reduced stress levels is tabulated in Table 2.

Table 2. Activation energies for recovery of creep resistant substructure

Reduced stress in psi σ_r	Activation energy after recovery, ΔH_r in kcal/mole	
500	135.0	[6]
2,500	105.0	(This investigation)
5,000	91.5	(This investigation)
7,500	77.0	(This investigation)

The fact that the observed recovery agrees satisfactorily with these values was demonstrated by the fact that when n for a given σ_r was plotted against θ_r [temperature compensated time for recovery = $t_r \exp(-\Delta H_r/RT)$] on log-log co-ordinates, all the data points fell on a common line, as shown in Figures 19, 20, and 21. The stress dependence of ΔH_r is shown in Figure 22.

Typical data giving the recovery parameter n as a function of time t_r, for recovery at 1020°C is shown in Figure 23. The stress dependence of n_{max} is shown in Figure 24. The intercept K of each curve in Figure 23 is plotted against the reduced stress σ_r in Figure 25.

Figure 26 is an optical micrograph of the (110) plane of an uncrept rutile sample. The dislocation density in an as-annealed condition is about 4×10^5 dislocations/cm^2.

Figure 27 is an optical micrograph of the (110) plane of a rutile specimen crept under a stress of 10,000 psi for 50 minutes at 1020°C and then furnace cooled under load. It may be observed that the dislocations climbed out of the slip plane to form subgrains at right angles to the $(1\bar{1}0)$ slip plane along $[1\bar{1}0]$ direction.

Figure 28 is an optical micrograph of a sample crept under the same conditions as that of Figure 27, but in this case the sample was given a subsequent recovery treatment under a reduced stress of 5,000 psi for 1 hour at the same test temperature. It may be seen that the formation of distinct subboundary walls was taken place with both an increase in their mean separation and a decrease in the density of dislocations in the region between the walls.

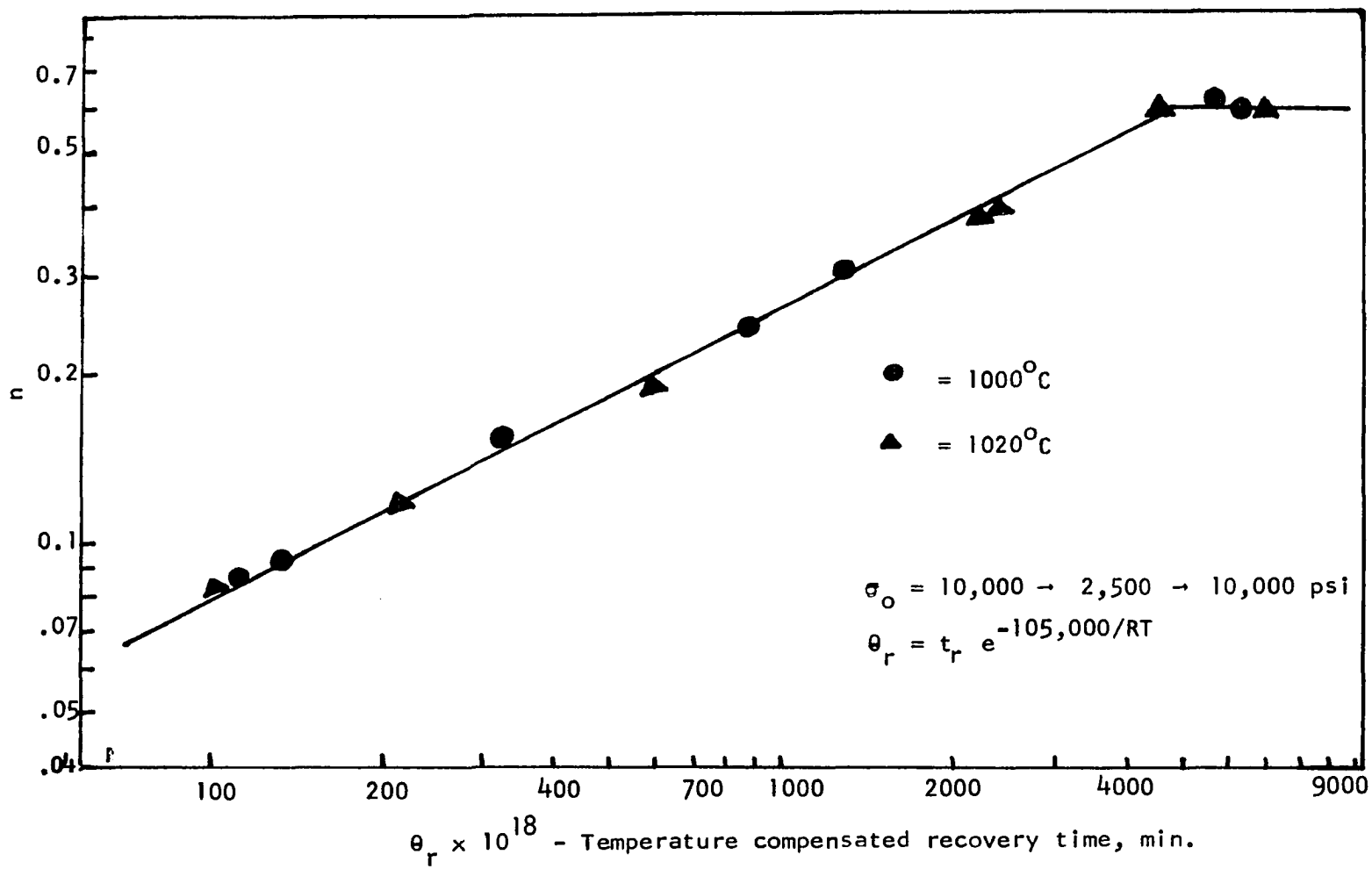

Figure 19. Thermal recovery of creep ability

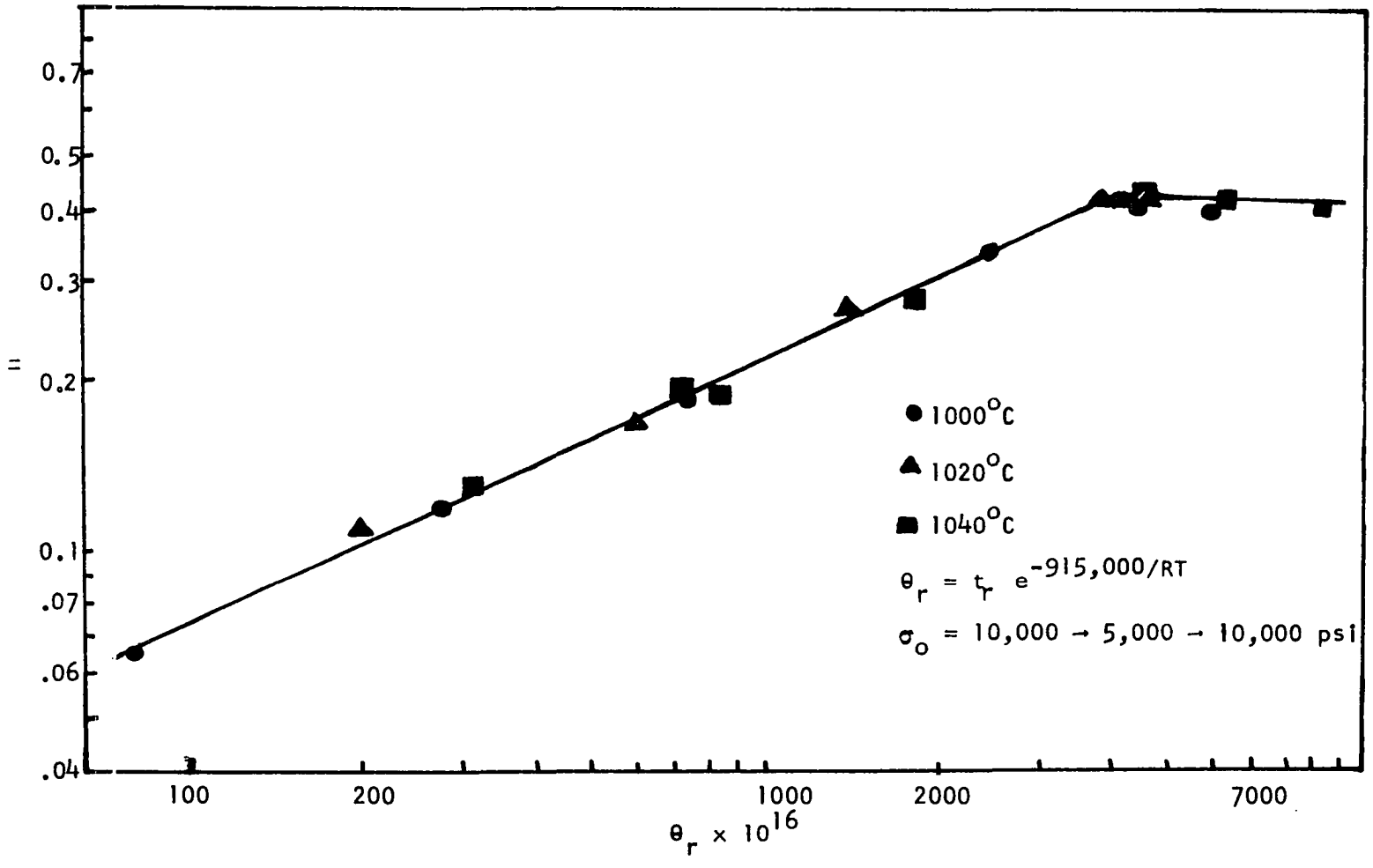

Figure 20. Thermal recovery of creep ability

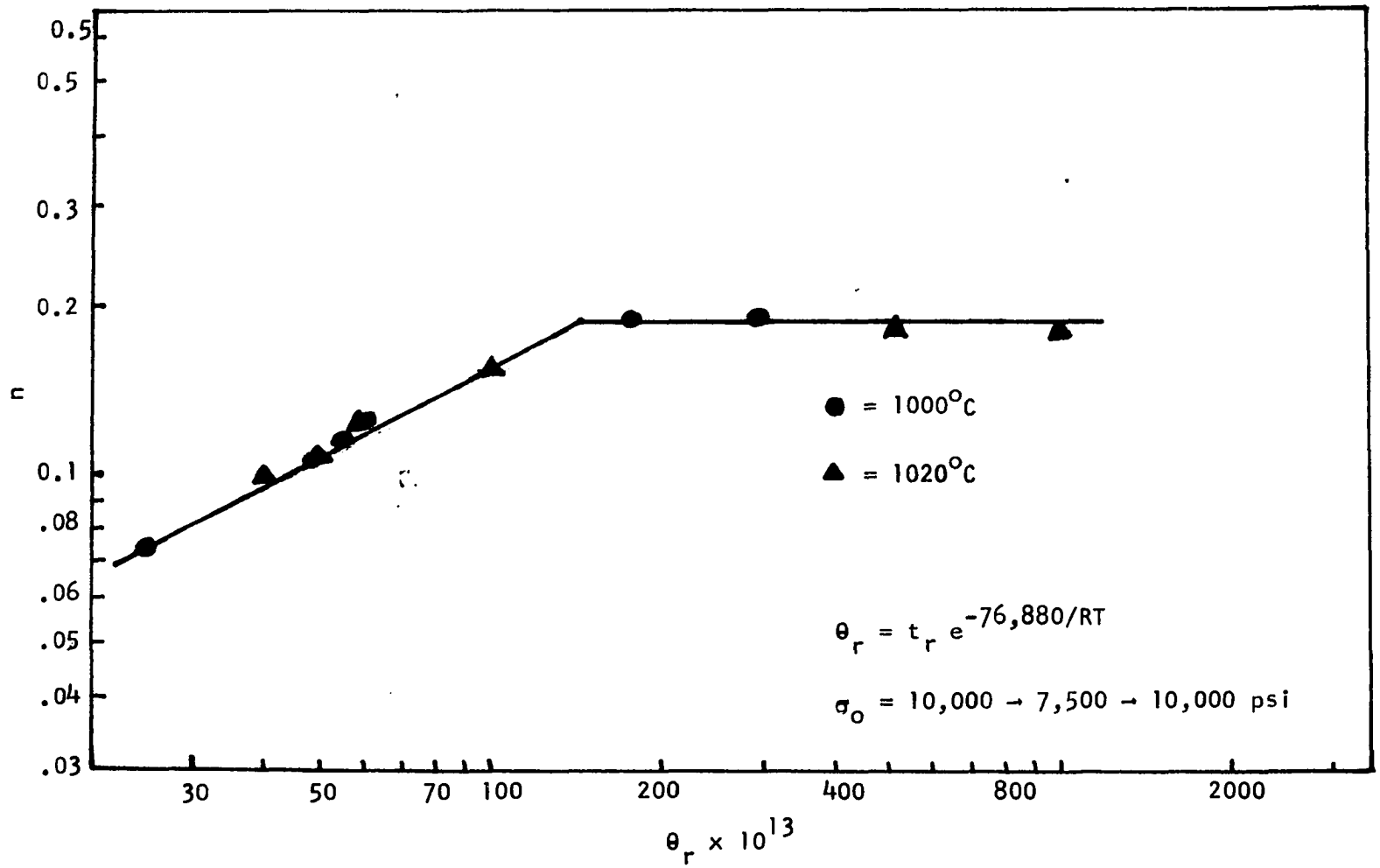

Figure 21. Thermal recovery of creep ability

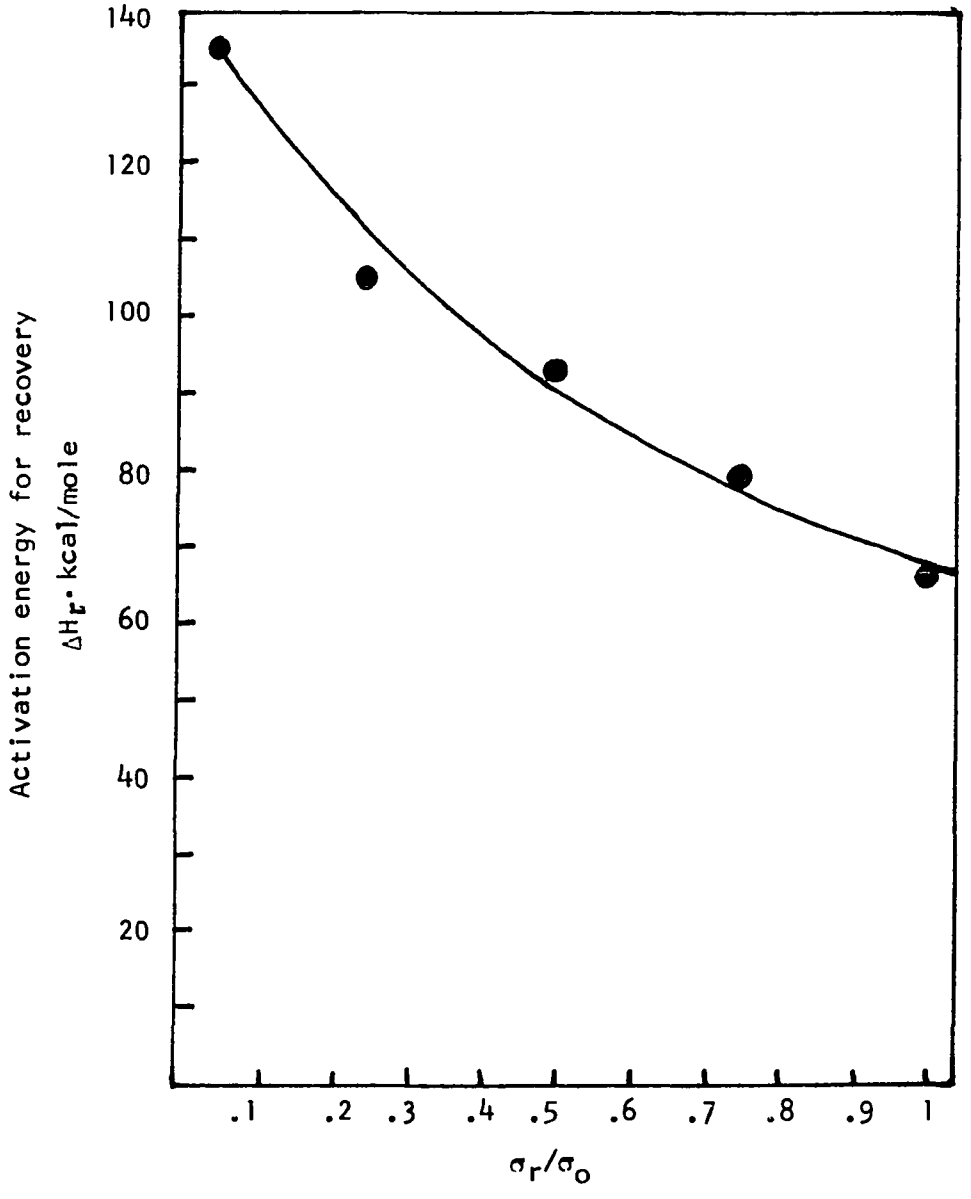

Figure 22. Activation energy for recovery vs σ_r/σ_o

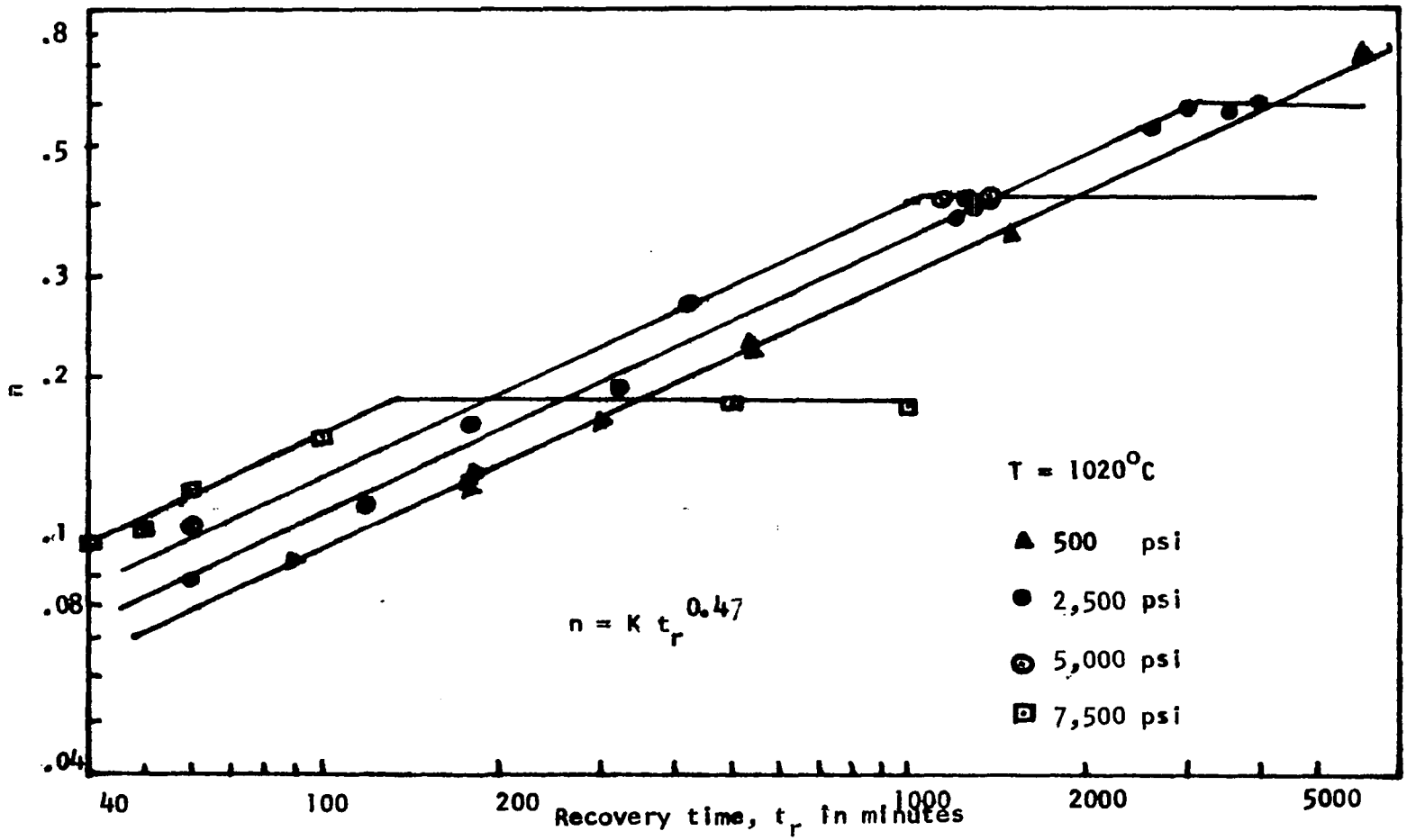

Figure 23. Creep recovery curves at 1020°C

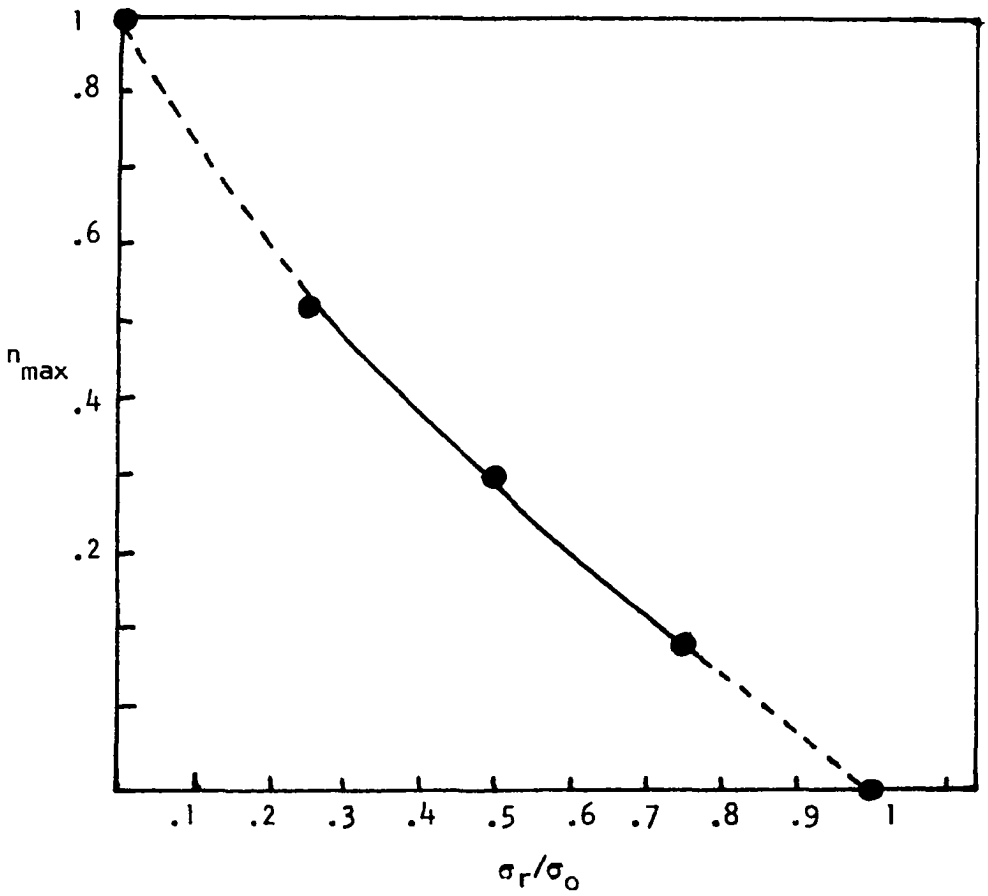

Figure 24. n_{max} vs σ_r/σ_o

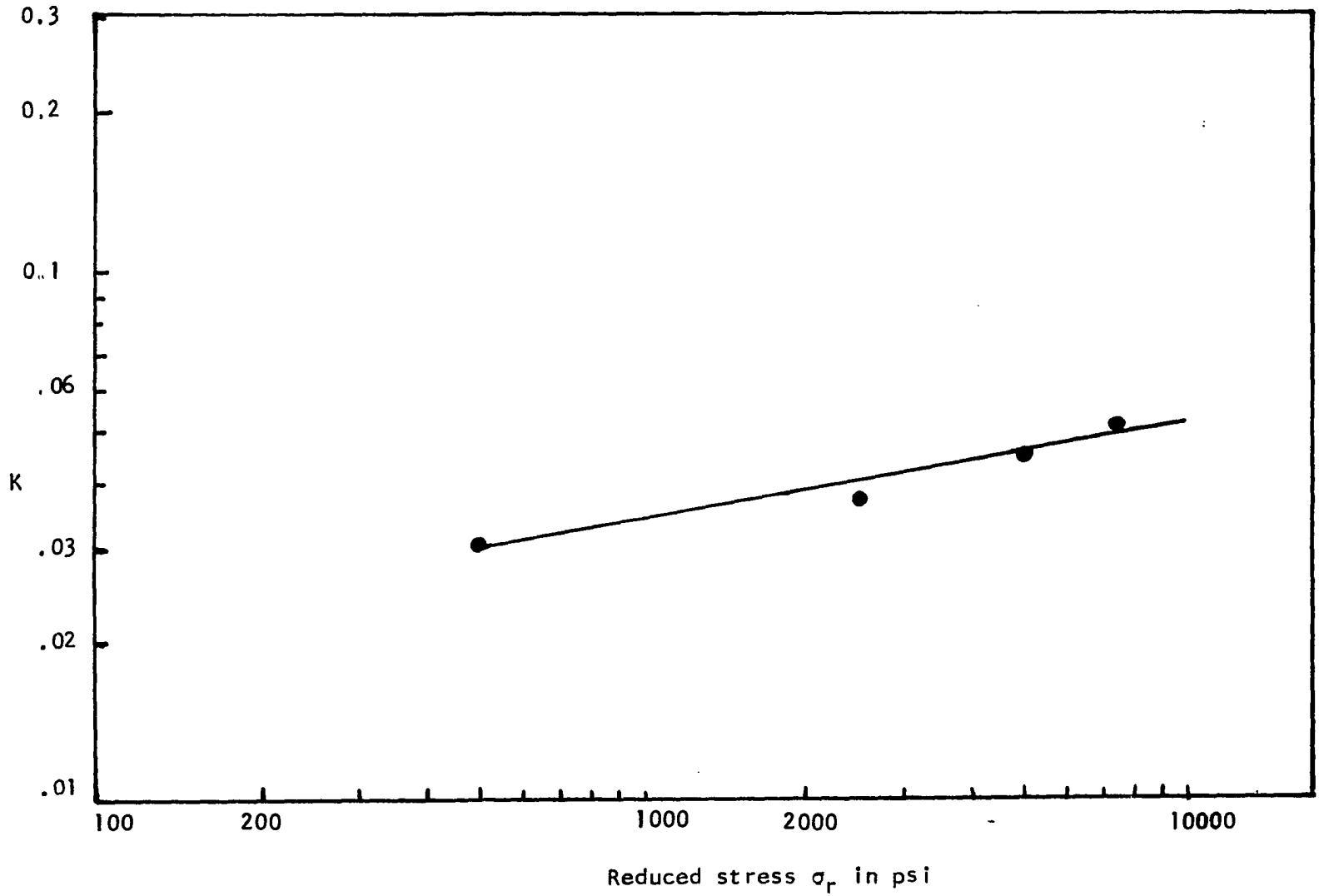

Figure 25. K vs σ_r

Figure 26. Dislocation configuration on the (110) face of uncrept rutile specimen (800x)

Figure 27. Dislocation configuration on the (110) face of rutile creep specimen crept for 50 minutes at 10,000 psi, 1020°C. No recovery treatment. (800x)

Arrow: $(1\bar{1}0)$ [001]

Figure 28. Dislocation configuration on the (110) face of rutile creep specimen crept for 50 minutes at 10,000 psi, 1020°C. Recovered for t_r = 1 hr at 5,000 psi, 1020°C. (800x)

Arrow: $(1\bar{1}0)$ [001]

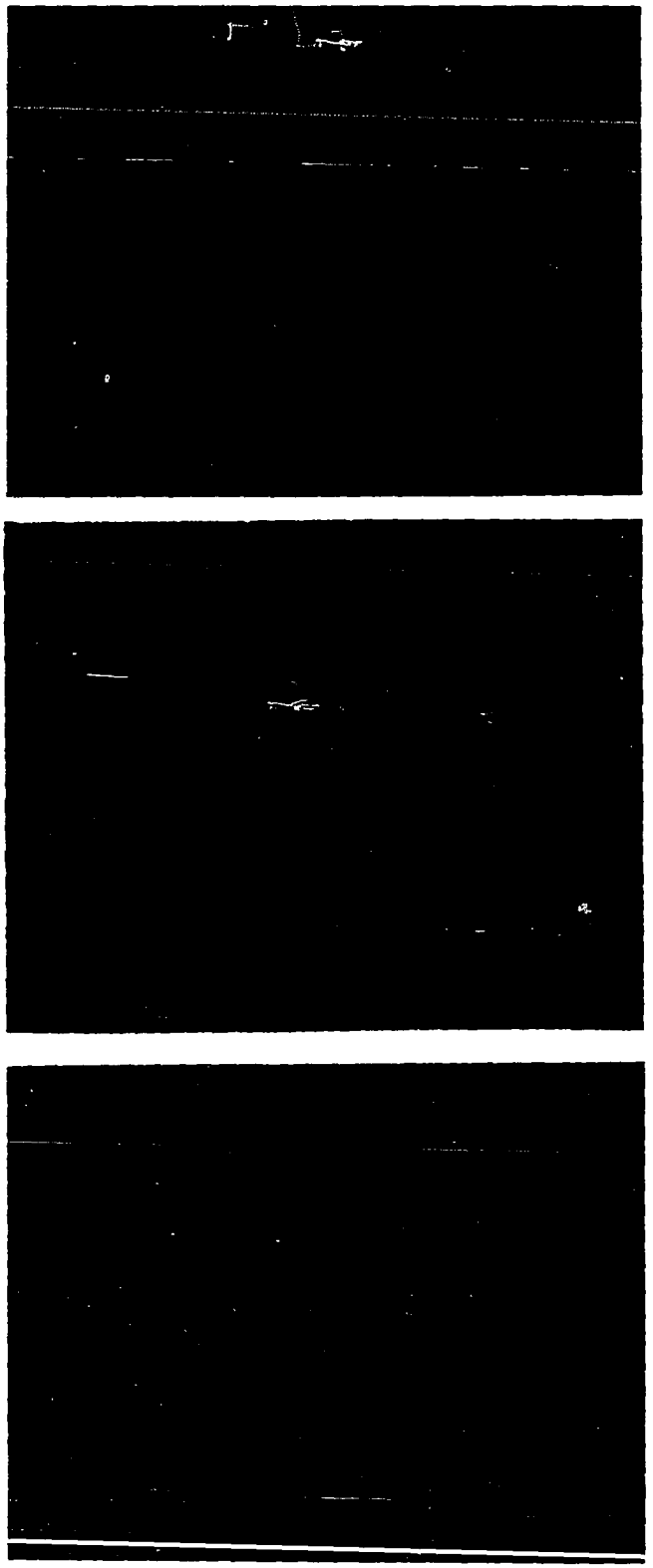

Figure 29 is an optical micrograph of the (110) face of a sample crept to the same conditions as in Figures 27 and 28, but given a more prolonged anneal of 9 hours at the same reduced stress (5,000 psi) and test temperature (1020°C). It may be seen the formation of very distinctive subboundary walls has taken place with an increase in their mean spacing. The dislocation walls became more distinct due to the more advanced rate of coalescence of dislocations.

Figure 30 is an optical micrograph of the (110) face of a sample crept to the same conditions as in Figure 27 and 28, but a given more prolonged anneal of 24 hours (in the early plateau region of n vs t_r plot, Figure 17) at the same reduced stress (5,000 psi) and test temperature (1020°C). It may be seen that an increase in the mean spacing of the dislocation walls and decrease in the dislocation density between the walls.

Figure 31 is an optical micrograph of the (110) face of a sample crept to the same conditions as in Figure 27, but given a more prolonged anneal of 48 hours (late plateau region of n vs tr plot, Figure 17) at the same reduced stress (5000 psi) and test temperature (1020°C). It may be seen that the mean spacing of the dislocation walls does not increase when compared with Figure 30.

Figure 32 is a typical example of a graph ρ, vs t_r, where ρ is the dislocation density within the subgrains. It may be observed that ρ decreases as the recovery time t_r is increased at a reduced stress of 5,000 psi at 1020°C. It may also be seen that the transition point t_r' in n vs t_r plot (Figure 17) corresponds to the transition point t_r' of the ρ vs t_r plot, (Figure 32).

Figure 29. Dislocation configuration on the (110) face of rutile creep specimen crept for 50 minutes at 10,000 psi, 1020°C. Recovered for t_r = 9 hrs at 5,000 psi, 1020°C. (800 x)

Arrow: $(1\bar{1}0)$ [001]

Figure 30. Dislocation configuration on the (110) face of rutile creep specimen crept for 50 minutes at 10,000 psi, 1020°C. Recovered for t_r = 24 hrs at 5,000 psi, 1020°C. (800 x)

Arrow: $(1\bar{1}0)$ [001]

Figure 31. Dislocation configuration on the (110) face of rutile creep specimen crept for 50 minutes at 10,000 psi, 1020°C. Recovered for t_r = 48 hrs at 5,000 psi, 1020°C. (800 x)

Arrow: $(1\bar{1}0)$ [001]

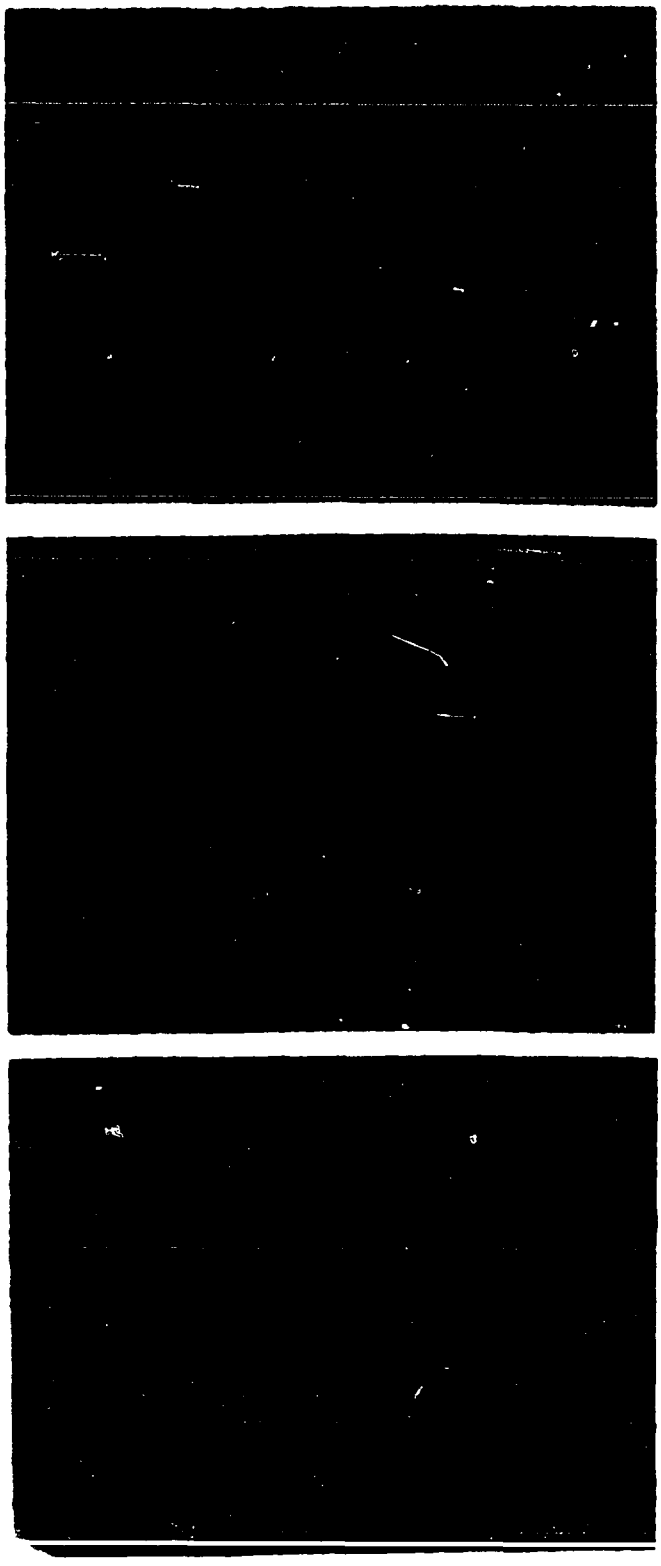

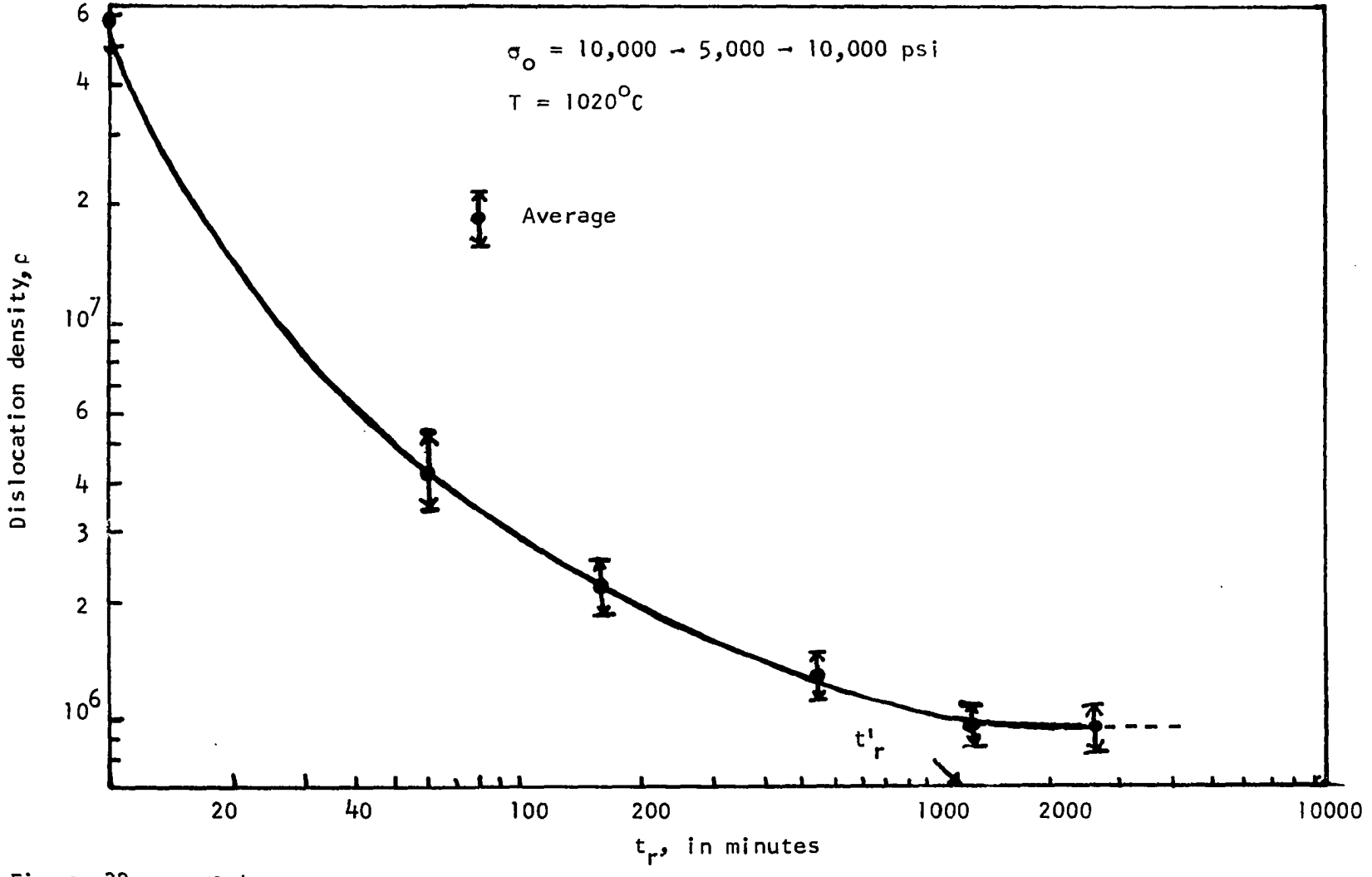

Figure 32. ρ vs t_r

V. DISCUSSION AND CONCLUSIONS

A. Discussion

Bell, Krishnamachari and Jones [6] have proposed a model on the recovery of high temperature creep resistant substructure in rutile. They suggested that the recovery mechanism involves the sweeping out of dislocation barriers within the material by the migration of dislocation walls or subgrain boundaries. Under constant stress conditions, subgrain walls usually play a passive role, and creep recovery is controlled by the climb of dislocations within the subgrains. When the stress is reduced, however, the subgrains tend to grow by subgrain boundary migration or coalescence because the reduced stress aids the thermal activation of the subboundary motion. These mobile dislocation walls can sweep up barriers to deformation within the original subgrains, which had to overcome by climb under constant stress conditions.

The dependence of the recovery parameter n on the recovery time t_r was shown by Bell et al. [6] to follow the relation

$$n = K\, t_r^{0.47} \tag{23}$$

at zero reduced stress, where K is a constant.

The above equation gives an excellent fit to the data obtained in Figures 16, 17, and 18, for recovery under reduced stresses of 2,500, 5,000 and 7,500 psi, until the maximum value of $n = n_{max}$ is obtained. At this maximum value the substructure coincides with that obtained for the secondary stage of creep under the reduced stress. This is evidenced by a constant dislocation density after the transition time, t_r', as shown in

Figure 32. Also the optical micrographs, Figures 30 and 31, show the constant substructure at $n = n_{max}$.

The factor K depends on the reduced stress σ_r. According to the recovery model as the reduced stress σ_r is increased the mobile dislocation walls must sweep up barriers for deformation much faster than at zero stress. This implies that the recovery per unit time should increase with increase in reduced stress. This trend was observed as shown in Figure 25 where the factor K increases with increase in reduced stress σ_r. That is, the recovery process is stress assisted and the Equation (23) may be written as

$$n = K\ (\sigma_r)\ t_r^{0.47}. \tag{24}$$

If recovery is due to a single thermally activated process having a constant activation energy, the Equation (23) can be written as

$$n = K_1\ \theta_r^{0.47} \tag{25}$$

where $\theta_r = t_r\ e^{-\Delta H_r/RT}$. When n is plotted against θ_r on log-log coordinates as shown in Figures 19, 20, and 21, all the points lie on the same curve. It justifies aposteriori the assumption that ΔH_r is insensitive to the test temperature and to the substructural changes attending recovery over the range of conditions under study. The parallelism of the curves in Figure 17 reveals that ΔH_r is constant for a given reduced stress. The activation energy for the recovery process depends on the reduced stress as shown in Figure 22. It suggests that the reduced stress σ_r aids the thermal activation to overcome the barriers

that are introduced during creep.

During high temperature creep there is a continual formation and recovery of creep resistant substructure. Throughout the primary stage of creep under constant stress and temperature, the rate of formation of the creep resistant substructure exceeds its rate of recovery, thereby causing the creep rate to decrease with time. During the secondary stage of creep, the rate of recovery must balance the rate of formation of the creep resistant substructure to provide a steady state creep rate. This suggests that the activation energy for recovery might coincide with that of creep. As documented extensively in the literature [12,13] and confirmed again by Bell, Krishnamachari and Jones [6], the activation energy for high temperature creep of near stoichiometric rutile is 66 kcal/mole. The observed activation energies under reduced stresses of 500, 2,500, 5,000 and 7,500 psi are respectively 135, 105, 91.5 and 77 kcal/mole. This clearly shows that when the recovery takes place under a reduced stress, the activation energy for recovery of creep resistant substructure is stress dependent and greater than 66 kcal/mole. The difference between the activation energies suggests the possibility that the method of measuring the extent of recovery by the reduced stress treatment was incorrectly formulated. However, the excellent correlation of the recovery parameter n, with $\theta_r = t_r e^{-\Delta H_r/RT}$ is evidence that the adopted procedure was valid. If the nature of the recovery upon reduction of stress depends on different substructural changes than those which take place upon recovery under a constant stress, then two different activation energies should be expected.

Under reduced stress, recovery due to climb from cells, entanglements and dipoles continues to take place. If this recovery were responsible for the recovery under reduced stress, however, the activation energy would be 66 kcal/mole independent of the applied stress. The higher activation energies for recovery under reduced stress, as cited in Table 2, clearly indicate that simultaneously another type of recovery process is occurring which is absent in a creep test under a constant stress.

Migration of subboundaries was observed illustrating the same general features previously noted by Bell et al. [6]. Optical micrographs, Figures 27 through 29, show that the dislocation walls have swept through a volume of the crystal since the average dislocation wall spacing has increased and the dislocation density has decreased.

These observations appear to be consistent with the model of Bell, Krishnamachari and Jones for the recovery of creep resistant substructure in rutile [6].

The reduced stress σ_r aids the thermal activation of the subgrain boundary motion. Washburn and Parker [53] reported in their work with zinc single crystals that thermal energy aided by the applied stress can bring about the collection of dislocations into sharp boundaries and subsequent subgrain boundary motion. That is, they observed stress induced motion of small angle or subgrain boundaries. Raymond and Dorn [44] in their work on the recovery of creep resistant substructure in aluminum have also suggested that the applied stress aids the thermal activation of the subboundary motion.

It can be assumed that as the dislocation walls slowly sweep out

volumes of the material they would leave in their wake what is essentially completely recovered material. The observed decrease in the dislocation density is not surprising since the dislocation walls would be expected to migrate in the direction of greatest dislocation density [37]. The more extensive creep including the partial recovery of primary creep upon reapplication of the original stress is believed to be due both to (1) the greater mobility of the remaining dislocations in the swept out region [19], and (2) the entry of other dislocations from adjacent unswept out regions into the recovered regions.

The mechanisms for the recovery of creep resistant substructure for both aluminum and rutile are the same. But in lead no such mechanism was observed. Several investigators have reported subgrain formation in aluminum [40,45,48], and rutile [6,25] during creep deformation. No such subgrain formation is observed in lead because of its low stacking fault energy [16].

The results of the recovery of creep resistant substructure on lead aluminum and rutile are tabulated in Table 3.

B. Conclusions

1. The creep resistance of rutile in the temperature range 1000 - 1040°C is reduced by reduced stress treatment. It is due to the recovery of creep resistant substructure.

2. The apparent activation energies for recovery are greater than the activation energy for creep, and are stress dependent.

3. Metallographic examination of etch pit configurations revealed that dislocation walls became distinct, the separation of walls increased

Table 3. Comparison of recovery process

Material	$\frac{T}{Tm}$	Reduced Stress σ_r psi	Activation energy for creep ΔH_c kcal/mole	Activation energy for recovery ΔH_r kcal/mole	Possible recovery process	Reference
1. Lead	0.07-0.18	0	18.4	19.8	Recrystallization	Kennedy [30]
2. Lead	0.15-0.18 -0.21	0	23.5	24	--	Bull [7]
3. Aluminum	0.42-0.47 -0.5	0	35.5	64	Migration of subboundaries	Ludemann et al. [36]
4. Aluminum	"	10 - 250 500 - 700	35.5	64-62-52 -37	"	Raymond and Dorn [44]
5. Rutile	0.54-0.56 -0.575	400	66	135	Migration of subboundary walls	Bell et al. [6]
6. Rutile	0.54-0.56 -0.575	2,500-5,000 -7,500	66	105-92-77	"	present study

and the density of dislocations decreased during the course of recovery.

4. These observations lead to the conclusion that the recovery process involves the coalescence of dislocations into subgrain boundaries or dislocation walls which then migrate through the sample sweeping up barriers to dislocation motion.

5. The recovery process is stress assisted although the maximum obtainable recovery decreases as the level of the reduced stress is increased.

VI. SUGGESTIONS FOR FURTHER STUDY

There are three areas of interest where further studies in rutile might be carried. They are:

1. Creep of non-stoichiometric rutile
2. Anelastic recovery of rutile
3. Thin film technique.

Deviation from stoichiometry may have a pronounced effect on creep. It might affect the plastic flow by altering the strength of the dislocation motion, or by influencing the interaction between vacancies and dislocations. Because of increase in the diffusivity, the deviation from stoichiometry would lower the high temperature creep resistance. Since the creep of near stoichiometric rutile was studied by several investigators [5,6,15,24,25], it is worthwhile to study the creep properties of non-stoichiometric rutile.

Relatively little experimental information is available to define the role of anelasticity in non-steady creep behavior. Since the probable mechanism of creep recovery was established in this investigation, it may be of interest to study the anelastic behavior of rutile.

In recent years the technique of electron transmission metallography has made it possible to examine the dislocation net works at sub-boundaries. Hirthe et al. [23] reported a technique for preparation of thin films of near-stoichiometric rutile by ion bombardment for transmission electron microscopy. Their technique might be used to get thin films of crept and recovered rutile specimens for electron microscope study. The nature of the substructural details after different creep and recovery histories could be studied.

VII. LITERATURE CITED

1. K. H. ASHBEE and R. E. SMALLMAN, J. Am. Ceram. Soc., 46 211 (1963).

2. C. R. BARRETT, Trans. AIME, 239 1726 (1967).

3. H. BELL, "The High-temperature Creep Characteristics of Aluminum 1.8 Atomic Percent Magnesium Solid Solution Under Conditions of: I. Constant Stress and Temperature, and II. With a Reduced Stress Treatment," Ph.D. dissertation, University of California, Berkeley (1966).

4. H. BELL, unpublished data.

5. H. BELL, V. KRISHNAMACHARI and J. JONES, J. Am. Ceram. Soc., 54 359 (1971).

6. H. BELL, V. KRISHNAMACHARI and J. JONES, "Recovery of High-temperature Creep Resistant Substructure in Rutile," ISU-ERI-99927 (1971), to be published in J. Am. Ceram. Soc.

7. J. BULL, "Recovery of the High-temperature Creep Resistant Substructure of Polycrystalline Lead," M.S. thesis, Iowa State University (1968).

8. R. W. CAHN, J. Inst. Met., 76 121 (1949).

9. B. CHALMERS, J. Inst. Met., 61 72 (1937).

10. C. Y. CHENG, A. KARIM, T. G. LAGDON and J. E. DORN, Trans. AIME, 242 890 (1968).

11. H. CONRAD, J. Metals, 16 582 (1964).

12. J. E. DORN, J. Mech. Phys. Solids., 3 85 (1954).

13. J. E. DORN, in Creep and Recovery, p. 255, ASM Seminar (1957).

14. J. E. DORN, Mechanical Behavior of Materials at Elevated Temperatures, McGraw-Hill, New York (1961).

15. N. E. FARB, O. W. JOHNSON and P. GIBBS, J. Appl. Phys. 36 1746 (1965).

16. F. GAROFALO, Fundamentals of Creep and Creep-Rupture in Metals, The Macmillan Co., New York (1965).

17. P. GAY, P. B. HIRSCH and A. KELLY, ActaCryst., 7 41 (1941).

18. R. C. GIFKINS, Trans. AIME, 215 1015 (1959).

19. J. H. GITTUS, Phil. Mag., 21 495 (1970).

20. F. A. GRANT, Revs. Mod. Phys., 31 646 (1959).

21. G. J. GUARNIERI, ASTM, Spec. Tech. Publication, 165 105 (1954).

22. W. R. HIBBARD, Acta Mett., 3 409 (1955).

23. W. M. HIRTHE, A. T. MELVILLE and P. H. WACKMAN, J. Am. Ceram. Soc., 49 454 (1966).

24. W. M. HIRTHE and J. O. BRITTAIN, J. Am. Ceram. Soc., 45 546 (1962).

25. W. M. HIRTHE and J. O. BRITTAIN, J. Am. Ceram. Soc., 46 411 (1963).

26. H. HU, Recovery and Recrystallization of Metals, L. Himmel, ed., p. 311, Interscience Publishers, New York (1963).

27. T. S. Ke, Phys. Rev., 71 533 (1947).

28. A. J. KENNEDY, Proceedings Royal Soc., 213A 492 (1952).

29. A. J. KENNEDY, British J. Appl. Phys., 4 225 (1953).

30. A. J. KENNEDY, Proceedings Royal Soc., 68 257 (1955).

31. A. J. KENNEDY, Process of Creep and Fatique in Metals, John Wiley and Sons, Inc., New York (1963).

32. T. G. LANGDON and J. A. PASK, High-temperature Oxides, Part III, A. M. Alper, ed., p. 53, Academic Press, New York and London (1970).

33. H. A. LEQUEAR and J. D. LUBAHN, ASTM, 126 163 (1952).

34. J. C. M. LI, J. Appl. Phys. 33 2958 (1962).

35. J. D. LUBAHN, J. of Metals, 7 103 (1955).

36. W. P. LUDEMANN, L. A. SHEPARD and J. E. DORN, Trans. AIME, 218 923 (1960).

37. K. LÜKE and K. DETERT, Acta Met., 5 628 (1957).

38. S. S. MANSON and W. F. BROWN, Jr., ASTM. Special Technical Publication, 260 65 (1959).

39. J. A. MARTIN, M. HERMAN and N. BROWN, Trans. AIME, 209 78 (1957).

40. D. McLEAN, J. Inst. Metals, 81 287 (1952).

41. N. F. MOTT, Phil. Mag., 43 1151 (1952).

42. A. K. MUKERJEE, J. E. BIRD and J. E. DORN, Trans. ASM, 62 155 (1969).

43. E. C. W. PERRYMAN, Acta Met., 2 26 (1954).

44. L. RAYMOND and J. E. DORN, Trans. AIME, 230 560 (1964).

45. I. S. SERVI, J. T. NORTON and N. J. GRANT, Trans. AIME, 194 965 71 (1952).

46. L. A. SHEPARD and J. E. DORN, "The Role of Subgrains in High-temperature Creep," UCB-IER-108 (1957).

47. O. D. SHERBY, T. A. TROZERA and J. E. DORN, Trans. ASTM, 56 789 (1956).

48. C. J. E. SMITH and I. L. DILLAMORE, Met. Science Journal, 4 161 (1970).

49. P. R. SWANN, Electron Microscopy and Strength of Crystals, John Wiley, p. 131 New York (1963).

50. R. A. VANDERMEER and P. GORDON, Recovery and Recrystallization of Metals, L. Himmel, ed., p. 211, Interscience Publishers, New York (1963).

51. J. B. WACHTMAN, Jr. and L. H. MAXWELL, J. Am. Ceram. Soc., 37 291 (1954).

52. J. B. WACHTMAN, Jr. and L. H. MAXWELL, J. Am. Ceram. Soc., 40 377 (1957).

53. J. WASHBURN and E. R. PARKER, Trans. AIME, 194 1076 (1952).

54. J. WEERTMAN, J. Appl. Phys., 26 1213 (1955).

55. J. WEERTMAN, J. Appl. Phys., 28 362 (1957).

56. S. WEISSMANN, Trans. ASM, 53 265 (1961).

57. S. WEISSMANN, T. IMURA and N. HOSOKAWA, Recovery and Recrystallization of Metals, L. Himmel, ed., p. 241 (1963).

58. D. H. WHITMORE and T. KAWAI, J. Am. Ceram. Soc., 45 375 (1962).

59. G. W. WILMS and W. A. WOOD, J. Inst. Metals, 75 693 (1948).

60. W. A. WOOD and R. F. SCRUTTON, J. Inst. Metals, 77 423 (1950).

61. W. A. WOOD and J. W. SUITER, J. Inst. Metals, 80 501 (1951).

62. C. ZENER, Elasticity and Anelasticity of Metals, The University of Chicago Press, Chicago (1948).

VIII. ACKNOWLEDGMENTS

In carrying out the work described in the foregoing pages, the author is indebted to the Engineering Research Institute of Iowa State University for providing a graduate assistantship. The author wishes to express his sincere appreciation to Dr. Howard Bell for his guidance and advice. Special thanks go to Dr. Glenn Murphy for his encouragement. Also the author is thankful to Dr. Jones, Dr. Roberts, and Dr. Peterson for sharing their thoughts with him.

The author is thankful to his late mother, Vinjamuri Venkatamma, for her valuable suggestion to go abroad for higher studies. He is also deeply indebted to his sister, Miss V. Ranga, who has helped him financially throughout his undergraduate and graduate studies. Last, but not least, he is thankful to his wife, V. Sarada, for her valuable companionship.